

Temporal Wasserstein Imputation: Versatile Missing Data Imputation for Time Series

Shuo-Chieh Huang

Department of Statistics, Rutgers University

Tengyuan Liang

Booth School of Business, University of Chicago

and

Ruey S. Tsay

Booth School of Business, University of Chicago

March 3, 2025

Abstract

Missing data can significantly hamper standard time series analysis, yet in practice they are frequently encountered. In this paper, we introduce temporal Wasserstein imputation, a novel method for imputing missing data in time series. Unlike existing techniques, our approach is fully nonparametric, circumventing the need for model specification prior to imputation, making it suitable for potential nonlinear dynamics. Its principled algorithmic implementation can seamlessly handle univariate or multivariate time series with any non-systematic missing pattern. In addition, the plausible range and side information of the missing entries (such as box constraints) can easily be incorporated. As a key advantage, our method mitigates the distributional bias typical of many existing approaches, ensuring more reliable downstream statistical analysis using the imputed series. Leveraging the benign landscape of the optimization formulation, we establish the convergence of an alternating minimization algorithm to critical points. We also provide conditions under which the marginal distributions of the underlying time series can be identified. Numerical experiments, including extensive simulations covering linear and nonlinear time series models and a real-world groundwater dataset laden with missing values, corroborate the practical usefulness of the proposed method.

Keywords: Optimal transport, Nonlinear time series, Threshold AR model, Compositional time series, Nonstationary time series

1 Introduction

In many scientific fields, data collection is often subject to various disruptions such as idiosyncratic or system-level instrument failures or changes in data collection policies, leading to missing entries in the data (Little and Rubin, 2019). In time series analysis, missing data pose serious challenges to the application of many statistical tools since it is typically presumed that observations are available at equally spaced time points. Moreover, since the dynamic relationship is of crucial importance in time series analysis, one cannot proceed by throwing away the missing data, even if the missing data appear completely at random (i.e., the missing pattern is independent of the series).

To tackle this issue, one approach is to impute the missing entries, after which the vast array of time series methods becomes readily applicable for statistical inference in the downstream. Naturally, the estimation of the *optimal interpolator*, which is the expectation of the missing data conditional on the observed data, has been extensively studied (Harvey and Pierse, 1984; Pourahmadi, 1989; Peña and Maravall, 1991; Gómez et al., 1999; Alonso and Sipols, 2008; Peña and Tsay, 2021; McElroy and Politis, 2020, 2022; McElroy, 2022). Since the optimal interpolator would depend on the probabilistic structure of the underlying process, most methods involve EM-type iterations that alternate between model identification and missing data imputation (see, for example, Chpt. 4 of Peña and Tsay, 2021). Besides the optimal interpolator, ad hoc deterministic imputation methods, such as smoothing with linear interpolation, B-splines and wavelets (see, for instance, Hastie et al., 2009), are also used in practice for their simplicity.

However, the optimal interpolator can cause distributional biases that are detrimental to downstream statistical analysis. To illustrate, consider an AR(1) process, $x_t = \phi x_{t-1} + \epsilon_t$, where $0 < |\phi| < 1$ and $\{\epsilon_t\}$ is a sequence of i.i.d. standard normal random variables. The optimal interpolator can be expressed in terms of the inverse autocorrelation functions (Peña and Maravall 1991; McElroy and Politis 2022; see also Chpt. 6 of Peña et al., 2011).

For instance, suppose that data at time indices T and $T + 1$ are missing. Then the optimal interpolators are given by

$$\hat{x}_T = \frac{\phi(1 + \phi^2)}{1 + \phi^2 + \phi^4}x_{T-1} + \frac{\phi^2}{1 + \phi^2 + \phi^4}x_{T+2}, \quad \hat{x}_{T+1} = \frac{\phi^2}{1 + \phi^2 + \phi^4}x_{T-1} + \frac{\phi(1 + \phi^2)}{1 + \phi^2 + \phi^4}x_{T+2}.$$

Using the fact that $\mathbb{E}(x_t x_{t-h}) = \phi^h / (1 - \phi^2)$, for $h \geq 0$, it is not difficult to show that

$$\mathbb{E}(\hat{x}_T^2) = \mathbb{E}(\hat{x}_{T+1}^2) = \frac{\phi^2 + 3\phi^4 + 3\phi^6 + 2\phi^8}{(1 + \phi^2 + \phi^4)^2} \mathbb{E}(x_t^2) < \mathbb{E}(x_t^2), \text{ and}$$

$$|\mathbb{E}(\hat{x}_T \hat{x}_{T+1})| = \frac{2\phi^2 + 3\phi^4 + 3\phi^6 + \phi^8}{(1 + \phi^2 + \phi^4)^2} |\mathbb{E}(x_t x_{t+1})| < |\mathbb{E}(x_t x_{t+1})|.$$

Hence, the variance and the autocovariances of the imputed data are different from those of the original AR(1) process. In general, the joint distribution of the optimally interpolated time series is often quite different from that of the original process, leading to questionable downstream statistical analysis, especially when the number of missing data is non-negligible. Similar biases are also observed for some deterministic imputation methods (Carrizosa et al., 2013).

In addition to the distributional bias, the above example also reveals further predicaments of the optimal interpolator. First, in order to compute the optimal interpolator, one often needs to choose a model class before imputation. However, such a decision relies heavily on domain expertise and may be ill-informed when there are many missing values. While it is possible, for certain time series models, to estimate the model parameters without imputation, it still engages in model specification before imputation. Second, it may be difficult to compute the optimal interpolator if some nonlinear model is employed. With different missing patterns and different chosen models, the computational procedure may change drastically. Finally, incorporating *side information* about the missing data into this methodology appears less straightforward. Side information about the missing data restricts the set of admissible imputations. For instance, a compositional time series is known to lie in $[0, 1]$ and sums to unity at each time point. Besides the optimal inter-

polator, many deterministic interpolators such as B-spline smoothing are also inclined to over-(or under-)shoot, leading to imputations that are outside plausible ranges.

In this paper, we present the temporal Wasserstein imputation (TWI), a novel approach for time series imputation which circumvents the aforementioned limitations. As a non-parametric method, TWI is highly versatile and can be applied to a wide range of time series data. In particular, as a key advantage of TWI, it requires no model class specification prior to imputation, allowing it to perform well even when the underlying time series is nonlinear, such as the threshold autoregressive processes (TAR, [Tong, 1983](#)). Formulated as an optimization problem, TWI can be implemented efficiently through an alternating minimization algorithm. This principled algorithmic approach allows for the seamless integration of side information by restricting the admissible imputations, and its extension to multivariate time series is also straightforward. The optimization and statistical underpinnings of TWI are closely related to the optimal transport problem ([Villani, 2008, 2021](#); [Cuturi, 2013](#)), which is briefly reviewed in [Section 2](#). [Section 3](#) maps out the optimization formulation and introduces the computational scheme in detail.

The core idea of TWI is that by minimizing the Wasserstein distance (over all admissible imputations) between the marginal distributions before and after a specified time point, the marginal distributions implied by the imputation shall resemble those of the original series, thereby lowering the distributional bias discussed above. In [Section 4](#), we investigate the optimization and statistical properties of TWI. Our analysis shows that the optimization landscape of TWI is biconvex and the alternating algorithm is guaranteed to converge to a critical point. However, from the statistical viewpoint, missing data imputation suffers from an identification issue: Many distributions (of the stochastic process) may be equally plausible in describing the corrupted series. This raises the question of whether and under what conditions TWI can identify the underlying marginal distributions. In [Section 4.2](#), we show, via a two-state Markov chain example, that the correct underlying distributions can

indeed be identified by TWI under assumptions on the missing pattern and the stability of the imputation. The latter condition motivates a simple modification of TWI, termed k -TWI, which shows further improvement in imputation quality from TWI in our numerical experiments.

In Section 5, we evaluate the performance of TWI on synthetic data generated from a wide range of time series models, including nonlinear, multivariate, and nonstationary settings. Across all processes considered, TWI successfully recovers the underlying dynamics and yields favorable downstream statistics such as autocovariance and model parameter estimates. Its advantage is particularly prominent in the presence of nonlinear dynamics. In Section 6, we apply TWI to a real-world groundwater dataset with many missing data. After imputation, we conduct independent component analysis and autoregressive modeling in the downstream. Compared to existing methods, TWI effectively captures the underlying dynamics, producing interpretable components as well as accurate autoregressive predictions. These numerical results support the practical contributions of TWI.

2 Preliminary: Optimal transport

In this section, we briefly review the optimal transport (OT) problem, which serves as a prerequisite to the rest of the paper. For a more comprehensive account on the theory of optimal transport, the readers are referred to Villani (2021, 2008).

Given two probability measures μ and ν defined on \mathbb{R}^p and a cost function $L : \mathbb{R}^p \times \mathbb{R}^p \rightarrow \mathbb{R}_+$, the optimal transport cost between μ and ν is defined as

$$\text{OTC}(\mu, \nu) = \inf_{\pi \in \mathcal{M}(\mu, \nu)} \int L(\mathbf{x}, \mathbf{y}) d\pi(\mathbf{x}, \mathbf{y}),$$

where \mathcal{M} is the set of couplings between μ and ν , i.e., probability measures over $\mathbb{R}^p \times \mathbb{R}^p$ with marginals μ and ν . The classic interpretation for the minimization problem is finding the most cost effective way to move a pile of earth distributed as μ (with volume normalized

to one) to fill a pit whose shape is distributed as ν . It also has a matching or assignment interpretation that has led to fruitful results in the economics literature ([Galichon, 2016](#)). If $L(\mathbf{x}, \mathbf{y}) = \|\mathbf{x} - \mathbf{y}\|^2$, where $\|\cdot\|$ is the usual Euclidean distance, and if μ is absolutely continuous with respect to the Lebesgue measure, then under some regularity conditions [Brenier \(1987\)](#) showed that the optimal coupling which attains the infimum is the push-forward measure of μ , $(\text{Id}, T)_\# \mu$, where $T : \mathbb{R}^p \rightarrow \mathbb{R}^p$ is unique μ -almost everywhere. The map T , called the optimal transport map, clearly satisfies $T_\# \mu = \nu$.

If $L(\mathbf{x}, \mathbf{y}) = \|\mathbf{x} - \mathbf{y}\|^k$, for some $k \geq 1$, the resulting optimal transport cost is known as the Wasserstein distance of order k (to the k -th power), which we formally denote as $\mathcal{W}_k(\mu, \nu)$. Namely,

$$\mathcal{W}_k(\mu, \nu) := \left\{ \inf_{\pi \in \mathcal{M}(\mu, \nu)} \int \|\mathbf{x} - \mathbf{y}\|^k d\pi(\mathbf{x}, \mathbf{y}) \right\}^{1/k} = \{\text{OTC}(\mu, \nu)\}^{1/k}.$$

The Wasserstein distance is a metric on the space of probabilities with finite k -th moment on \mathbb{R}^p , and metrizes the weak topology on this space ([Villani, 2021](#), Chpt. 9). In particular, if μ and $\{\mu_t : t = 1, 2, \dots\}$ are probability measures on \mathbb{R}^p such that $\mathcal{W}_k(\mu_t, \mu) \rightarrow 0$ as $t \rightarrow \infty$, then $\mu_t \Rightarrow \mu$ and $\int \|\mathbf{x}\|^k \mu_t(d\mathbf{x}) \rightarrow \int \|\mathbf{x}\|^k \mu(d\mathbf{x})$, where \Rightarrow denotes the weak convergence of probability measures ([Billingsley, 1995](#)). Therefore, it can be used as a discrepancy metric between μ and ν . In fact, the Wasserstein distance offers several advantages over other discrepancy metrics such as the Kullbeck-Leibler divergence and the Kolmogorov-Smirnov distance. For instance, the Wasserstein distance has a nice dual representation and handles support mismatch easily, making it suitable for machine learning and statistical applications.

If μ and ν are discrete measures, for instance $\mu = \sum_{i=1}^n p_i \delta_{\mathbf{x}_i}$ and $\nu = \sum_{j=1}^m q_j \delta_{\mathbf{y}_j}$, where $\{\mathbf{x}_i\}_{i=1}^n, \{\mathbf{y}_j\}_{j=1}^m$ are in \mathbb{R}^p , $\sum_{i=1}^n p_i = \sum_{j=1}^m q_j = 1$, $p_i > 0$, $q_j > 0$ for all i, j , and $\delta_{\mathbf{x}}$ denotes the dirac measure at \mathbf{x} , then the minimization problem becomes the following

linear program.

$$\begin{aligned} \text{OTC}(\mu, \nu) = & \min_{\{\pi_{ij}\}, \pi_{ij} \geq 0} \sum_{i,j} L(\mathbf{x}_i, \mathbf{y}_j) \pi_{ij} \\ \text{s.t. } & \sum_{i=1}^n \pi_{ij} = q_j, \quad j = 1, \dots, m, \quad \sum_{j=1}^m \pi_{ij} = p_i, \quad i = 1, \dots, n. \end{aligned} \quad (1)$$

The constraints in (1) enforce the joint distribution $\{\pi_{ij}\}$ to be a coupling between μ and ν , and will henceforth be called the coupling constraints. In the discrete case, the optimal coupling $\{\pi_{ij}\}$ typically involves split of masses for discrete measures and is no longer the push-forward under an one-to-one map. Recent research has made significant progress in the fast computation of the solution $\{\pi_{ij}\}$ through entropic regularization and some algorithms are amenable to large-scale parallelization and can be accelerated with GPUs; see [Cuturi \(2013\)](#) and [Peyré and Cuturi \(2019\)](#).

3 Temporal Wasserstein imputation

In this section, we introduce the proposed temporal Wasserstein imputation (TWI) method for time series imputation. First, we provide an optimization formulation of the proposed method that directly connects to the optimal transport problem. Then, we describe an alternating minimization algorithm to impute the missing values. The algorithm also reveals some connections between the proposed method and some existing approaches.

3.1 Optimization formulation

Let $\{\tilde{x}_t\}$ be the time series of interest and we observe the time series $\{x_t : t = 0, 1, \dots, n-1\}$. Denote by \star a generic missing value, and \mathcal{M} the set of time indices corresponding to the missing observations. Thus, $x_t = \star$ if $t \in \mathcal{M}$ and $x_t = \tilde{x}_t$ otherwise. We discuss below the case that x_t is stationary. The case of unit-root nonstationary series is discussed at the end of this section. If $\{\tilde{x}_t\}$ is stationary, then its p -dimensional marginal distribution μ_p , i.e. the distributions of $(\tilde{x}_t, \tilde{x}_{t-1}, \dots, \tilde{x}_{t-p+1})$, does not depend on t , where

$p \in \mathbb{N}$. In view of this property, when imputing the missing values in (x_0, \dots, x_{n-1}) , we seek an imputation $\mathbf{w} = (w_0, w_1, \dots, w_{n-1})^\top$ whose marginal distribution remains nearly unchanged. More specifically, we first split the time series into two parts $\{w_0, w_1, \dots, w_{n_1}\}$ and $\{w_{n_1+1}, w_{n_1+2}, \dots, w_{n-1}\}$ and define the two empirical marginal distributions

$$\hat{\mu}_{\text{pre}}(\mathbf{w}) = \sum_{t=p-1}^{n_1} \frac{\delta_{(w_t, w_{t-1}, \dots, w_{t-p+1})}}{n_1 - p + 2}, \quad \hat{\mu}_{\text{post}}(\mathbf{w}) = \sum_{t=n_1+1}^{n-1} \frac{\delta_{(w_t, w_{t-1}, \dots, w_{t-p+1})}}{n - n_1 - 1},$$

where $p-1 < n_1 < n-p$, and the values of p and n_1 used will be discussed later. The discrepancy between the two empirical distributions can then be measured by the optimal transport cost, which is the minimum value of the following linear program.

$$\text{OTC}(\hat{\mu}_{\text{pre}}(\mathbf{w}), \hat{\mu}_{\text{post}}(\mathbf{w})) = \left. \begin{aligned} & \min_{\mathbf{\Pi}=(\pi_{ij})_{ij}, \pi_{ij} \geq 0} \sum_{i=p-1}^{n_1} \sum_{j=n_1+1}^{n-1} \pi_{ij} L(\mathbf{v}_i(\mathbf{w}), \mathbf{v}_j(\mathbf{w})) \\ & \text{s.t.} \quad \sum_{i=p-1}^{n_1} \pi_{ij} = \frac{1}{n - n_1 - 1} \quad \text{for all } j \\ & \quad \sum_{j=n_1+1}^{n-1} \pi_{ij} = \frac{1}{n_1 - p + 2} \quad \text{for all } i, \end{aligned} \right\} \quad (2)$$

where $\mathbf{v}_i(\mathbf{w}) := (w_i, w_{i-1}, \dots, w_{i-p+1})^\top$, and, for ease of notation, we enumerate the rows and columns of the $(n_1 - p + 2) \times (n - n_1 - 1)$ matrix $\mathbf{\Pi}$ by $\{p-1, p, \dots, n_1\}$ and $\{n_1+1, \dots, n-1\}$, respectively. An important special case of (2) is when $L(\mathbf{v}_i(\mathbf{w}), \mathbf{v}_j(\mathbf{w})) = \|\mathbf{v}_i(\mathbf{w}) - \mathbf{v}_j(\mathbf{w})\|^k$, for some $k \geq 1$. In this case, we have $\text{OTC}(\hat{\mu}_{\text{pre}}, \hat{\mu}_{\text{post}}) = \mathcal{W}_k^k(\hat{\mu}_{\text{pre}}, \hat{\mu}_{\text{post}})$.

Our goal is to find the imputation that minimizes the aforementioned discrepancy. Thus, we solve for

$$\hat{\mathbf{w}} := (\hat{w}_0, \dots, \hat{w}_{n-1})^\top = \arg \min_{\mathbf{w} \in \mathcal{C}} \text{OTC}(\hat{\mu}_{\text{pre}}(\mathbf{w}), \hat{\mu}_{\text{post}}(\mathbf{w})), \quad (3)$$

where the constraint set \mathcal{C} delineates the admissible imputations. Typically, it enforces the imputation to agree with the observed data, in which case $\mathcal{C} = \{\mathbf{w} : w_t = x_t, t \notin \mathcal{M}\}$. It may also reflect the *side information* available. For example, if x_t are monthly sales data, the knowledge of quarterly sales define a set of linear constraints for the missing values. Another example is when $\{\mathbf{x}_t\}$ is a d -dimensional compositional time series such

as the market share of several companies in an industry. It follows that $\mathbf{x}_t^\top \mathbf{1} = 1$ for all t . Then, by defining $\mathcal{C} = \{\mathbf{W} \in \mathbb{R}^{n \times d} : \mathbf{W}\mathbf{1}_d = \mathbf{1}_n\}$, where $\mathbf{1}_n = (1, \dots, 1)^\top \in \mathbb{R}^n$, the set of admissible imputations are restricted to be compositional as well.

One may also consider the following regularized version of (3).

$$\hat{\mathbf{w}} := (\hat{w}_0, \dots, \hat{w}_{n-1})^\top = \arg \min_{\mathbf{w} \in \mathcal{C}} \left\{ \text{OTC}(\hat{\mu}_{\text{pre}}(\mathbf{w}), \hat{\mu}_{\text{post}}(\mathbf{w})) + \frac{\lambda}{2} \|\mathbf{w}\|^2 \right\}, \quad (4)$$

where the regularization parameter $\lambda > 0$ is small. As we will see in the next subsection, the ℓ_2 -regularization term makes a subproblem in the alternating minimization algorithm strongly convex, enhancing numerical stability. In addition, in the important special case corresponding to the Wasserstein distance of order 2, i.e., $L(\mathbf{v}_i(\mathbf{w}), \mathbf{v}_j(\mathbf{w})) = \|\mathbf{v}_i(\mathbf{w}) - \mathbf{v}_j(\mathbf{w})\|^2$, the regularization allows one to solve the subproblem by finding a fixed point of a linear system. Since L is often chosen to be some power of the Euclidean norm, which induces the Wasserstein distances between the marginal distributions of a time series, the solution $\hat{\mathbf{w}}$ to (3) or (4) is called the temporal Wasserstein imputation (TWI) throughout this paper.

In this formulation, it is clear that the temporal Wasserstein imputation, which seeks to equate the marginal distributions on both sides of n_1 , is nonparametric. With a mildly large p , the p -dimensional marginal distributions can sometimes fully characterize the nonlinear dynamics of a Markov process (such as a finite-order threshold AR process), which would otherwise need many parameters using ARMA approximation.

3.2 Alternating minimization algorithm

The optimization landscapes of (3) and (4) are complicated because the optimal transport cost is itself the minimum value of a linear program (2), and there are potentially many variables to optimize. To tackle this issue, we propose to solve the nested minimization problem using alternating minimization. Since (3) is a special case of (4) with $\lambda = 0$, we focus our discussion on (4).

To begin, observe that with an initialized $\hat{\mathbf{w}}^{(0)}$, problem (2) is exactly the discrete optimal transport problem. Thus, at iteration $k = 1, 2, \dots$, treating $\mathbf{w} = \hat{\mathbf{w}}^{(k-1)}$ as fixed, we may compute the optimizer $\hat{\Pi}^{(k)}$ of (2) efficiently by some existing algorithms (Cuturi, 2013; Peyré and Cuturi, 2019). This corresponds to the inner optimization problem of (4). Next, we optimize (4) over \mathbf{w} , taking $\Pi = \hat{\Pi}^{(k)}$ as fixed. This procedure is repeated until convergence. Let

$$F(\mathbf{w}, \Pi) = \sum_{i=p-1}^{n_1} \sum_{j=n_1+1}^{n-1} \pi_{ij} L(\mathbf{v}_i(\mathbf{w}), \mathbf{v}_j(\mathbf{w})) + \frac{\lambda}{2} \|\mathbf{w}\|^2, \quad (5)$$

and the procedure described above can be summarized in Algorithm 1. One advantage of the alternating minimization scheme is that the subproblems (steps (a) and (b) in Algorithm 1) are easy to optimize when L satisfies some regularity conditions. Optimization guarantees are discussed in the next subsection.

Algorithm 1: Temporal Wasserstein imputation with alternating minimization

Input: Cut-off n_1 , number of lags p

Initialization: $\mathbf{w}^{(0)} \in \mathcal{C}$

1 **for** $k = 1, 2, \dots$ **do**

2 Step (a): Solve for $\hat{\Pi}^{(k)}$ in problem (2), treating $\mathbf{w} = \hat{\mathbf{w}}^{(k-1)}$ as fixed.

3 Step (b): Solve for $\hat{\mathbf{w}}^{(k)} \in \arg \min_{\mathbf{w} \in \mathcal{C}} F(\mathbf{w}, \hat{\Pi}^{(k)})$.

4 **Break** if convergence criterion is met and set $\hat{\mathbf{w}} = \hat{\mathbf{w}}^{(k)}$

5 **end**

Output: Imputed time series $\hat{\mathbf{w}}$

Next, we investigate the properties of Algorithm 1 in an important special case where closed forms can be obtained. Suppose $L(\mathbf{v}_i, \mathbf{v}_j) = \|\mathbf{v}_i - \mathbf{v}_j\|^2$. Then it is not difficult to show that $F(\mathbf{w}, \Pi) = \mathbf{w}^\top \mathbf{H}(\Pi) \mathbf{w}$, where $\mathbf{H}(\Pi) = \sum_{h=0}^{p-1} \mathbf{A}_h(\Pi) + \frac{\lambda}{2} \mathbf{I}_n$ and

$$\mathbf{A}_h(\Pi) = \begin{pmatrix} \mathbf{0}_{p-1-h} & & & \\ & \frac{1}{n_1-p+2} \mathbf{I}_{n_1-p+2} & -\Pi & \\ & -\Pi^\top & \frac{1}{n-n_1-1} \mathbf{I}_{n-n_1-1} & \\ & & & \mathbf{0}_h \end{pmatrix} \in \mathbb{R}^{n \times n}, \quad h = 0, 1, \dots, p-1,$$

in which all unspecified entries in $\mathbf{A}_h(\boldsymbol{\Pi})$ are zero, and $\mathbf{0}_h$ is an $h \times h$ matrix of zeros. Hence F is quadratic in \mathbf{w} . In fact, it can be shown that $\mathbf{H}(\boldsymbol{\Pi})$ is nonnegative definite for any $\boldsymbol{\Pi}$ satisfying the coupling constraints. Moreover, F is strongly convex in \mathbf{w} if $\lambda > 0$ (see also Proposition 3 in Section 4). Thus many efficient solvers are applicable in this step (Boyd and Vandenberghe, 2004; Parikh et al., 2014). If, in addition, the constraint set \mathcal{C} is defined through a system of linear equations, i.e., $\mathcal{C} = \{\mathbf{w} \in \mathbb{R}^n : \mathbf{K}\mathbf{w} = \mathbf{b}\}$ for some known \mathbf{K} and \mathbf{b} , then step (b) in Algorithm 1 has the following closed form

$$\hat{\mathbf{w}}^{(k)} = \mathbf{H}^{-1}\mathbf{K}^\top(\mathbf{K}\mathbf{H}^{-1}\mathbf{K}^\top)^{-1}\mathbf{b}, \quad (6)$$

where $\mathbf{H} = \mathbf{H}(\hat{\boldsymbol{\Pi}}^{(k)})$.

Suppose further that $\mathcal{C} = \{\mathbf{w} : w_t = x_t, t \notin \mathcal{M}\}$. That is, there is no side information about the missing values. In this case, the solution $(\hat{w}_0, \dots, \hat{w}_{n-1})$ to the subproblem in step (b) must satisfy the following system of linear equations which has the same number of unknowns and equations.

$$\left\{ \begin{array}{l} \hat{w}_s = \frac{\sum_{i=s \vee (p-1)}^{s+p-1} \sum_{j=n_1+1}^{n-1} \hat{\pi}_{ij} \hat{w}_{j-i+s}}{\frac{p \wedge (s+1)}{n_1-p+2} + \frac{\lambda}{2}}, \quad \text{if } 0 \leq s \leq n_1 - p + 1, s \in \mathcal{M} \\ \hat{w}_s = \frac{\sum_{i=s}^{n_1} \sum_{j=n_1+1}^{n-1} \hat{\pi}_{ij} \hat{w}_{j-i+s} + \sum_{i=p-1}^{n_1} \sum_{j=n_1+1}^{s+p-1} \hat{\pi}_{ij} \hat{w}_{i-j+s}}{\frac{n_1-s+1}{n_1-p+2} + \frac{s+p-n_1+1}{n-n_1-1} + \frac{\lambda}{2}}, \\ \quad \text{if } n_1 - p + 2 \leq s \leq n_1, s \in \mathcal{M} \\ \hat{w}_s = \frac{\sum_{i=p-1}^{n_1} \sum_{j=s}^{(s+p-1) \wedge (n-1)} \hat{\pi}_{ij} \hat{w}_{i-j+s}}{\frac{p \wedge (n-s)}{n-n_1-1} + \frac{\lambda}{2}}, \quad \text{if } n_1 + 1 \leq s \leq n - 1, s \in \mathcal{M} \\ \hat{w}_s = x_s, \quad \text{if } s \notin \mathcal{M} \end{array} \right. \quad (7)$$

where $\hat{\boldsymbol{\Pi}} = (\hat{\pi}_{ij})$ is treated as fixed. We make a few remarks regarding (7).

Remark 1. Let us contrast TWI with the optimal interpolator. (7) shows, in general, the temporal Wasserstein imputation is a linear function of *many* observed data $\{x_t : t \notin \mathcal{M}\}$, even when p is small. On the other hand, the optimal interpolator is usually a linear combination of nearby observed data when the underlying process is a finite-order AR

model. For instance, suppose the underlying time series is an AR(1) process: $x_t = \phi x_{t-1} + \epsilon_t$, where $\{\epsilon_t\}$ is a mean-zero, unit-variance white noise. If $x_{n_1} = \star$ is the only missing value in the time series, then the optimal interpolator (Peña and Maravall, 1991) of x_{n_1} is

$$w_{n_1, \text{opt}} = \frac{\phi}{1 + \phi^2} (x_{n_1-1} + x_{n_1+1}).$$

In contrast, (7) shows that the temporal Wasserstein imputation (with $p = 2$ and $\lambda = 0$) is given by

$$\hat{w}_{n_1} = \frac{1}{n_1^{-1} + (n - n_1 - 1)^{-1}} \left(\sum_{t=0}^{n_1-1} \hat{\pi}_{t+1, n_1+1} x_t + \sum_{t=n_1+1}^{n-1} \hat{\pi}_{n_1, t} x_t \right),$$

which is a convex combination of all observed values. This is somewhat expected because, as a nonparametric method, TWI uses all data to learn the underlying dynamics.

Remark 2. (EM interpretation) Let $(\hat{\mathbf{w}}, \hat{\mathbf{\Pi}})$ be a fixed point of the alternating minimization algorithm (Algorithm 1). That is,

$$\hat{\mathbf{w}} \in \arg \min_{\mathbf{w} \in \mathcal{C}} F(\mathbf{w}, \hat{\mathbf{\Pi}}), \quad \hat{\mathbf{\Pi}} \in \arg \min_{\mathbf{\Pi}} F(\hat{\mathbf{w}}, \mathbf{\Pi}).$$

In addition, suppose $\lambda = 0$ for a moment. Let $\mathbf{u} = (u_0, u_1, \dots, u_{p-1})$ be a random vector whose distribution is $\hat{\mu}_{\text{pre}}$ and $\mathbf{v} = (v_0, \dots, v_{p-1})$ a random vector whose distribution is $\hat{\mu}_{\text{post}}$. Furthermore, let the joint distribution of (\mathbf{u}, \mathbf{v}) be given by the optimal transport coupling between $\hat{\mu}_{\text{pre}}$ and $\hat{\mu}_{\text{post}}$, identified as $\hat{\mathbf{\Pi}}$ (by viewing it as a joint distribution between the two discrete measures). Consider an index $s \in \mathcal{M}$ with $p-1 \leq s \leq n_1 - p + 1$. By (7), it is not difficult to see that

$$\begin{aligned} \hat{w}_s &= \frac{1}{p} \sum_{i=s}^{s+p-1} \sum_{j=n_1+1}^{n-1} \frac{\hat{\pi}_{ij}}{\sum_{j=n_1+1}^{n-1} \hat{\pi}_{ij}} \hat{w}_{j-i+s} \\ &= \frac{1}{p} \sum_{h=0}^{p-1} \mathbb{E}_{\hat{\mathbf{\Pi}}} (v_h | \mathbf{u} = (\hat{w}_{s+h}, \dots, \hat{w}_s, \dots, \hat{w}_{s+h-p+1})). \end{aligned} \quad (8)$$

(8) shows that the temporal Wasserstein imputation \hat{w}_s is essentially an average of conditional expectations. Thus, Algorithm 1 is closely related to the EM algorithm: To minimize

the Wasserstein distance $\mathbb{E}_{\Pi} \|\mathbf{u} - \mathbf{v}\|^2$, step (b) computes the conditional expectations under the current optimal transport coupling $\hat{\Pi}$ while step (a) minimizes over the coupling space. Formula like (8) can be derived for other time indices s with appropriate modifications.

Because of the optimization formulation, it is straightforward to extend TWI to multivariate time series. Suppose the multivariate time series of interest is $\mathbf{x}_t = (x_{t,1}, \dots, x_{t,d})^\top$. To compute the imputation $\mathbf{W} = (\mathbf{w}_0, \mathbf{w}_1, \dots, \mathbf{w}_{n-1})$ where $\mathbf{w}_t = (w_{t,1}, \dots, w_{t,d})^\top$, we may replace $\mathbf{v}_i(\mathbf{w})$ in (2) by $\mathbf{v}_i(\mathbf{W}) := (w_{i,1}, \dots, w_{i-p+1,1}, w_{i,2}, \dots, w_{i-p+1,2}, \dots, w_{i-p+1,d})^\top$. Then Algorithm 1 can still be applied. Since the multivariate information is summarized by the distance matrix $\mathbf{L} = (l_{ij})_{0 \leq i \leq n_1, n_1+1 \leq j \leq n-1}$, where $l_{ij} = L(\mathbf{v}_i(\mathbf{W}), \mathbf{v}_j(\mathbf{W}))$, regardless of the dimension d , step (a) in Algorithm 1 is identical as the scalar case. In the notable special case where $L(\mathbf{u}, \mathbf{v}) = \|\mathbf{u} - \mathbf{v}\|^2$, (5) becomes

$$F(\mathbf{W}, \Pi) = \sum_{l=1}^d \sum_{i=p-1}^{n_1} \sum_{j=n_1+1}^{n-1} \pi_{ij} \left[\sum_{h=0}^{p-1} (w_{i-h,l} - w_{j-h,l})^2 \right] + \frac{\lambda}{2} \|\mathbf{W}\|_F^2,$$

where $\|\cdot\|_F$ is the Frobenius norm. Straightforward calculations show that fixing $\Pi = \hat{\Pi}$, if $\hat{\mathbf{W}}$ is a solution to step (b) of Algorithm 1, then for each $l \in \{1, 2, \dots, d\}$, $(\hat{w}_{0,l}, \hat{w}_{1,l}, \dots, \hat{w}_{n-1,l})$ also satisfies the system of linear equations (7) in the case of no side information. Therefore, in step (b) of Algorithm 1, each component in the multivariate time series can be imputed in parallel to lower the computational overhead and only the values of individual series are involved in computing the imputation in each component. The cross-sectional information is exploited when learning the optimal transport coupling in step (a). Thus, the algorithm is fast to implement in the multivariate setting.

We shall compare TWI with the approach proposed by Carrizosa et al. (2013), which also aims to alleviate the corrupted statistical patterns caused by imputation. Their method is based on penalizing the deviation of some moments from the theoretical values. As a result, the moments, such as the autocorrelation functions, of the imputed series are close to the pre-specified values. However, this approach has a number of drawbacks. First, good theoretical values for the moments may not be readily available in practice, especially when

the missing values are many. Second, their approach promotes smoothness of the time series and hence positive autocorrelation, which does not necessarily align with the underlying time series. Finally, the optimization problem is highly non-convex, leading to an intense computational hurdle. In contrast, the proposed TWI is data-driven, completely nonparametric, and enjoys the computational advantages brought by the alternating minimization algorithm and recent advances in computational optimal transport.

Next, we discuss the imputation of nonstationary time series. For an $I(1)$ process $\{x_t\}$, $y_t = x_t - x_{t-1}$ is stationary and one can apply imputation methods to the first-differenced series $\{y_t\}$. More generally, one can apply TWI to the series $y_t = \phi(B)x_t$, where $\phi(z) = (1 - z)^d$ if x_t is an $I(d)$ process, and B is the back-shift operator. Then, an imputation for x_t can be recovered by inverting $\phi(B)$. Note that, in this case, the number of missing data in $\{y_t\}$ multiplies, and we need at least $d + 1$ contiguous observed values in $\{x_t\}$ to obtain an observed value for $\{y_t\}$. To mitigate the information loss, we can encode the information from the raw data via the admissible set \mathcal{C} . For example, consider the $I(1)$ case: If x_t is observed, then since $y_1 + \dots + y_t = x_t - x_0$, we may restrict the imputation $\{w_t\}$ for $\{y_t\}$ to satisfy $w_1 + \dots + w_t = x_t - x_0$ (assuming x_0 is observed). Finally, although we have motivated TWI from the stationarity of the underlying process, TWI fares quite well with certain nonstationary processes such as cyclic time series. In Section 5, we further explore the application of TWI to nonstationary time series.

4 Theoretical properties

In this section, we investigate the optimization and statistical properties of TWI. We first show Algorithm 1 converges to critical points. Then, asymptotic consistency of TWI is established when the missing data concentrate on one side of n_1 . For general non-systematic missing patterns, we show that identification of the underlying marginal distributions can be achieved by TWI under the assumptions of interpolator stability using a two-state

Markov chain example (see (C1) and (C2) in Section 4.2).

Before presenting the results, it is worthwhile to clarify the asymptotic regime under consideration. The analysis is meaningful only when the number of missing entries is non-negligible compared to the sample size. Otherwise, if $\sharp(\mathcal{M}) = o(n)$, where $\sharp(E)$ is the cardinality of the set E , then the empirical marginal distributions of any (bounded) imputations satisfy

$$\frac{1}{n} \sum_{t \in \mathcal{A}_n} \delta_{(w_t, w_{t-1}, \dots, w_{t-p+1})} + \frac{1}{n} \sum_{t \notin \mathcal{A}_n} \delta_{(w_t, w_{t-1}, \dots, w_{t-p+1})} \Rightarrow \mu_p,$$

where $\mathcal{A}_n = \{t \in \{p-1, \dots, n-1\} : \{t, t-1, \dots, t-p+1\} \cap \mathcal{M} \neq \emptyset\}$. Therefore, assuming $\sharp(\mathcal{M}) = o(n)$ would essentially preclude distributional inconsistency in the downstream. To avoid this trivial case, in this paper we maintain instead the assumption that $\mathcal{M} = \mathcal{M}_n$ is a sequence of index sets (independent of the underlying time series) such that $\sharp(\mathcal{M}_n)/n \asymp 1$, where $a_n \asymp b_n$ means there exists $0 < \underline{c} < \bar{c} < \infty$ such that $\underline{c} \leq a_n/b_n \leq \bar{c}$ for all large n .

4.1 Optimization and statistical guarantees

We begin by studying the optimization properties of Algorithm 1. All proofs are relegated to Section S1 of the supplementary material.

Proposition 3. *Suppose \mathcal{C} is a convex set and $F(.,.)$ is defined in (5). Then,*

$$(a) \text{ (monotonicity) } F(\hat{\mathbf{w}}^{(t)}, \hat{\mathbf{\Pi}}^{(t+1)}) \leq F(\hat{\mathbf{w}}^{(t)}, \hat{\mathbf{\Pi}}^{(t)}) \leq F(\hat{\mathbf{w}}^{(t-1)}, \hat{\mathbf{\Pi}}^{(t)}), t = 1, 2, \dots;$$

$$(b) \text{ every limit point } (\hat{\mathbf{w}}, \hat{\mathbf{\Pi}}) \text{ of } \{(\hat{\mathbf{w}}^{(t+1)}, \hat{\mathbf{\Pi}}^{(t)}) : t = 1, 2, \dots\} \text{ is a critical point of } F. \text{ i.e.,}$$

$$\frac{\partial F(\hat{\mathbf{w}}, \hat{\mathbf{\Pi}})}{\partial \mathbf{w}} \cdot (\mathbf{w} - \hat{\mathbf{w}}) \geq 0, \quad \frac{\partial F(\hat{\mathbf{w}}, \hat{\mathbf{\Pi}})}{\partial \text{vec}(\mathbf{\Pi})} \cdot \text{vec}(\mathbf{\Pi} - \hat{\mathbf{\Pi}}) \geq 0$$

for any $\mathbf{w} \in \mathcal{C}$ and $\mathbf{\Pi}$ satisfying the coupling constraints.

If, in addition, the cost function L takes the form $L(\mathbf{u}, \mathbf{v}) = \sum_{k=1}^p \ell(u_k - v_k)$, where $\mathbf{u} = (u_1, \dots, u_p)^\top$, $\mathbf{v} = (v_1, \dots, v_p)^\top$, and ℓ is twice differentiable and convex, then

(c) $F(\mathbf{w}, \mathbf{\Pi})$ is biconvex in \mathbf{w} and $\mathbf{\Pi}$.

Due to the biconvexity of F , one can employ off-the-shelf solvers for the subproblems in Algorithm 1. Moreover, it follows directly from the proof that if $\lambda > 0$, $F(\mathbf{w}, \mathbf{\Pi})$ is λ -strongly convex in \mathbf{w} . Hence, step (b) in Algorithm 1 admits a unique solution in each iteration and can be solved efficiently.

A few remarks are in order. First, it is straightforward to generalize Proposition 3 for multivariate time series. Second, like most methods involving non-convex optimization, a good initialization is crucial for converging to a “good” critical point. In our simulation studies, we use simple linear interpolation or ARIMA-based Kalman smoothing as initializations and TWI is able to find an imputation that offers substantial improvements over these initializations. Third, unlike many non-convex optimization problems, we are not satisfied by an arbitrary global minimizer of F . Essentially, it is because among all processes that have stable p -dimensional marginal distributions, only a subset of them matches the underlying marginal distributions. In Section 4.2, we probe this identification issue in more detail. However, when the missing data happen to lie on the same side of $t = n_1$, the global minimizer of F achieves asymptotic consistency in the sense of Proposition 4 below.

Proposition 4. *Assume (A1) and (A2) in Section S1 of the supplementary material. Suppose for any $\mathbf{w} \in \mathcal{C}$, $w_t = \tilde{x}_t$ if $t \notin \mathcal{M}_n$. Suppose further n and n_1 satisfy $n_1 \rightarrow \infty$ and $n - n_1 \rightarrow \infty$. If either $\mathcal{M}_n \subseteq \{0, 1, \dots, n_1\}$ or $\mathcal{M}_n \subseteq \{n_1 + 1, \dots, n - 1\}$ (but not both), then, the global minimizer $(\hat{\mathbf{w}}, \hat{\mathbf{\Pi}})$ of F with $\lambda = 0$ and $L(\mathbf{u}, \mathbf{v}) = \|\mathbf{u} - \mathbf{v}\|^k$, subject to $\mathbf{w} \in \mathcal{C}$ and the coupling conditions, satisfies*

$$\mathcal{W}_k \left(\frac{1}{n_1 - p + 2} \sum_{t=p-1}^{n_1} \delta_{\mathbf{v}_t(\hat{\mathbf{w}})}, \mu_p \right) + \mathcal{W}_k \left(\frac{1}{n - n_1 - 1} \sum_{t=n_1+1}^{n-1} \delta_{\mathbf{v}_t(\hat{\mathbf{w}})}, \mu_p \right) \rightarrow 0 \quad \text{almost surely.}$$

Proposition 4 implies the empirical marginal distributions of the imputed time series converge to the underlying marginal distribution in the Wasserstein distance. This implies $\hat{\mu}_{\text{pre}}(\hat{\mathbf{w}}) \Rightarrow \mu_p$ and $\hat{\mu}_{\text{post}}(\hat{\mathbf{w}}) \Rightarrow \mu_p$. Moreover, convergence in Wasserstein distance further

ensures for any continuous function φ with $|\varphi(x)| \leq C(1+|x|^k)$ for all $x \in \mathbb{R}$ and some $C < \infty$, we have $\int \varphi d\hat{\mu}_n \rightarrow \int \varphi d\mu$, where $\hat{\mu}_n$ is either $\hat{\mu}_{\text{pre}}(\hat{\mathbf{w}})$ or $\hat{\mu}_{\text{post}}(\hat{\mathbf{w}})$ (Villani, 2021). For such functionals $F_\varphi(\mu) = \int \varphi d\mu$, the temporal Wasserstein imputation provides consistent downstream statistics.

4.2 General missing pattern: A two-state Markov chain example

In this subsection, the identification issue of the temporal Wasserstein imputation method is studied via a two-state Markov chain example. Particularly, we connect the non-identification of the underlying marginal distributions to the lack of uniqueness of the solutions to a system of linear equations. We also show that, under two natural conditions, the correct marginal distributions can still be pinned down by TWI. To free our discussion from finite-sample complications, we will focus on the distribution level in this subsection, or intuitively speaking, assume “infinite sample.”

Suppose the underlying time series $\{\tilde{x}_t\}_{-\infty < t < \infty}$ under study is a two-state Markov chain. Specifically, $\tilde{x}_t \in \{0, 1\}$ and the transition probabilities are given by

$$\mathbb{P}(\tilde{x}_t = 1 | \tilde{x}_{t-1} = 0) = 0.6, \quad \mathbb{P}(\tilde{x}_t = 0 | \tilde{x}_{t-1} = 1) = 0.2.$$

The transition probabilities are specified to facilitate discussions, but the main results below are not specific to these choices. It is easy to check that $\{\tilde{x}_t\}$ has the stationary distribution given by $\mathbb{P}(\tilde{x}_t = 1) = 0.75$ and $\mathbb{P}(\tilde{x}_t = 0) = 0.25$. Consequently, the 2-dimensional marginal distribution of $\{\tilde{x}_t\}$ is specified by

$$\begin{aligned} \mathbb{P}((\tilde{x}_t, \tilde{x}_{t-1}) = (1, 1)) &= 0.6, & \mathbb{P}((\tilde{x}_t, \tilde{x}_{t-1}) = (1, 0)) &= 0.15, \\ \mathbb{P}((\tilde{x}_t, \tilde{x}_{t-1}) = (0, 1)) &= 0.15, & \mathbb{P}((\tilde{x}_t, \tilde{x}_{t-1}) = (0, 0)) &= 0.1. \end{aligned} \tag{9}$$

Without loss of generality, we set $n_1 = 0$. Suppose that before time n_1 , there is a missing value every q_1 observations. Likewise, there is a missing value every q_2 observations after time n_1 . Specifically, $x_t = \star$ if $-t$ is a positive integer multiple of q_1 , and similarly, $x_t = \star$

if t is a positive integer multiple of q_2 , where q_1 and q_2 are some integers larger than 2 and $q_1 \neq q_2$ (see condition (C1) below). Next, suppose an imputation $\{\hat{w}_t\}_{-\infty < t < \infty}$ has been made such that if $t < n_1$,

$$\begin{aligned}\mathbb{P}((\hat{w}_t, \hat{w}_{t-1}) = (1, 1) | (x_t, x_{t-1}) = (\star, 1)) &= a_1, \\ \mathbb{P}((\hat{w}_t, \hat{w}_{t-1}) = (1, 0) | (x_t, x_{t-1}) = (\star, 0)) &= b_1,\end{aligned}\tag{10}$$

and if $t \geq n_1$,

$$\begin{aligned}\mathbb{P}((\hat{w}_t, \hat{w}_{t-1}) = (1, 1) | (x_t, x_{t-1}) = (\star, 1)) &= a_2, \\ \mathbb{P}((\hat{w}_t, \hat{w}_{t-1}) = (1, 0) | (x_t, x_{t-1}) = (\star, 0)) &= b_2,\end{aligned}\tag{11}$$

for some $a_1, a_2, b_1, b_2 \in [0, 1]$. Note that \mathbb{P} in (10) and (11) should be interpreted as proportions since the imputation may depend on the whole sequence of $\{x_t\}$, and it is assumed that they are well-defined. Essentially, here we parametrize all imputation methods by a_1, a_2, b_1, b_2 , which correspond to different 2-dimensional marginal distributions. Indeed, from (9)–(11), we can compute the 2-dimensional marginal distributions of the imputed series. For $\{\hat{w}_t\}_{-\infty < t < 0}$,

$$\begin{aligned}\mathbb{P}((\hat{w}_t, \hat{w}_{t-1}) = (1, 1)) &= 0.6(1 - \frac{1}{q_1}) + \frac{3a_1}{4q_1}, \quad \mathbb{P}((\hat{w}_t, \hat{w}_{t-1}) = (1, 0)) = 0.15(1 - \frac{1}{q_1}) + \frac{b_1}{4q_1}, \\ \mathbb{P}((\hat{w}_t, \hat{w}_{t-1}) = (0, 1)) &= 0.15(1 - q_1^{-1}) + \frac{3}{4q_1}(1 - a_1), \\ \mathbb{P}((\hat{w}_t, \hat{w}_{t-1}) = (0, 0)) &= 0.1(1 - q_1^{-1}) + \frac{1}{4q_1}(1 - b_1).\end{aligned}$$

For $\{\hat{w}_t\}_{0 \leq t < \infty}$, we can obtain similar expressions with a_1, b_1, q_1 replaced by a_2, b_2, q_2 . The “correct” imputation should calibrate a_i ’s and b_i ’s such that the resulting 2-dimensional marginal distributions equal the marginal distribution of the underlying series, given in (9).

To achieve such identification, the correct imputation must choose

$$a_1^* = a_2^* = 0.8, \quad b_1^* = b_2^* = 0.6.\tag{12}$$

Note that this calibration does not depend on q_1, q_2 ; it only depends on the distributional properties of the underlying process.

Assuming the optimization is carried out perfectly¹, the temporal Wasserstein imputation (with $p \geq 2$) calibrates $a_i, b_i, i = 1, 2$, by equating the 2-dimensional marginal distributions of $\{\hat{w}_t\}_{-\infty < t < 0}$ and $\{\hat{w}_t\}_{0 \leq t < \infty}$. Hence, $\{a_1, a_2, b_1, b_2\}$ satisfies

$$\left. \begin{aligned} 0.6(1 - q_1^{-1}) + \frac{3}{4q_1}a_1 &= 0.6(1 - q_2^{-1}) + \frac{3}{4q_2}a_2, \\ 0.15(1 - q_1^{-1}) + \frac{1}{4q_1}b_1 &= 0.15(1 - q_2^{-1}) + \frac{1}{4q_2}b_2, \\ 0.15(1 - q_1^{-1}) + \frac{3}{4q_1}(1 - a_1) &= 0.15(1 - q_2^{-1}) + \frac{3}{4q_2}(1 - a_2), \\ 0.1(1 - q_1^{-1}) + \frac{1}{4q_1}(1 - b_1) &= 0.1(1 - q_2^{-1}) + \frac{1}{4q_2}(1 - b_2). \end{aligned} \right\} \quad (13)$$

If $q_1 = q_2$, then any imputation with $a_1 = a_2$ and $b_1 = b_2$ would satisfy (13). Naturally, identification is not possible in this case, which leads to our first condition.

(C1) Non-systematic missing pattern: $q_1 \neq q_2$.

Condition (C1) precludes the special case of down-sampling, which is notoriously hard to be treated as a missing data problem.

However, (C1) is inadequate for identification because the equations in (13) are not linearly independent. The lack of uniqueness of the solutions to (13) is at the crux of the identification problem in imputation. The blue lines in Figure 1 plots the set of solutions to (13). Each point on the blue line represents a legitimate TWI imputation whose marginal distributions before and after time n_1 are the same. Nonetheless, (12) hints an additional requirement for the correct imputation, giving rise to the following condition.

(C2) Interpolator stability: $a_1 = a_2, b_1 = b_2$.

Intuitively, (C2) requires that, given the same neighboring observations, one should impute the missing entries in the same way (at least probabilistically) before and after n_1 . Together, (C1) and (C2) imply a unique solution to the system (13) and are sufficient for identification.

¹This is where we ignore finite sample complications and assume a zero Wasserstein loss is achieved. One may use, for example, the hamming distance $L(x, y) = \mathbf{1}\{x \neq y\}$ as the ground metric for the discrete data.

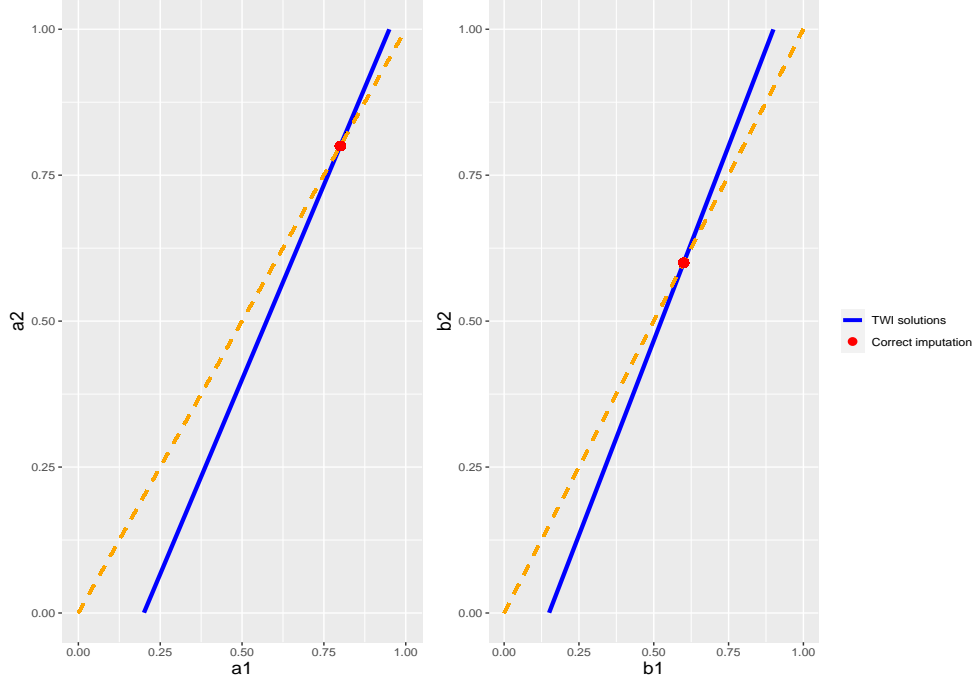


Figure 1: Set of calibrations that correspond to temporal Wasserstein imputation solutions (blue line) and the correct calibrations (a_1^*, a_2^*) and (b_1^*, b_2^*) (red dots). The dashed orange line is the 45 degree line. $q_1 = 3$ and $q_2 = 4$ are used to plot this figure.

Proposition 5. *Under (C1) and (C2), the only solution to (13) is*

$$a_1 = a_2 = a_1^*, \quad b_1 = b_2 = b_1^*.$$

*That is, the **only** 2-dimensional marginal distribution that achieves zero Wasserstein loss and satisfies (C2) is that of the underlying distribution.*

As shown in Figure 1, the 45 degree line (dashed orange), which imposes (C2), intersects with the solution set of temporal Wasserstein imputations at the correct calibrations. This example shows, under two natural requirements, TWI can achieve distributional identification through minimizing the Wasserstein distance between the marginal distributions.

In practice, appropriate tuning of n_1 and p is needed for TWI to find an imputation with marginal distributions approximating the underlying ones. As shown in Proposition 5, it is not necessary to use an n_1 such that all missing data lie on the same side. Instead, we can select n_1 from a pre-specified interval $[t_1, t_2]$ which yields the smallest Wasserstein

Algorithm 2: k -TWI

Input: Cut-off points n_1, n_2, \dots, n_k , number of lags p

Initialization: $\hat{\mathbf{w}}^{(0)} \in \mathcal{C}$

1 **for** $h = 1, 2, \dots, k$ **do**

2 Run Algorithm 1 with initialization $\hat{\mathbf{w}}^{(0)}$ and cut-off n_h to obtain $\hat{\mathbf{w}}$

3 Set $\hat{\mathbf{w}}^{(0)} = \hat{\mathbf{w}}$

4 **end**

Output: Imputed time series $\hat{\mathbf{w}}$

loss, where $t_2 - t_1$, t_2 , and $n - t_1$ are sufficiently large. Alternatively, a simple procedure to promote interpolator stability, as suggested by (C2), is to run TWI with different cut-off n_1 , using previously obtained imputations as initializations. This procedure, which we call k -TWI, is summarized in Algorithm 2. Finally, as a nonparametric method, p can be chosen to diverge with the sample size with $p/n \rightarrow 0$.

5 Simulation Studies

In this section, we apply TWI to data generated from various time series models, including multivariate, nonlinear, and nonstationary ones, to examine its performance. For comparison, we employ imputation methods such as Kalman smoothing, the scalar filtering algorithm of Peña and Tsay (2021), and deterministic methods such as linear and spline interpolations. In addition, the following two missing patterns are considered.

Pattern I: 300 observations are omitted at random;

Pattern II: For every 20 observations, 6 consecutive observations are omitted.

Pattern I simulates sporadic missing data while Pattern II generates patches of missing data. The total length of the time series is set to $n = 1000$. Thus, for both missing patterns, 30% of the data are missing. For each data generating process and missing pattern considered, 1000 Monte Carlo simulations are carried out.

We employ the proximal gradient descent (Parikh et al., 2014) to efficiently solve step (b) in Algorithm 1 when no side information is available since the projection step is straightforward. Conversely, when \mathcal{C} is defined by a system of linear equations, we solve step (b) using the closed form (6). Throughout we fix $n_1 = 0.4n$ and $p = 6$ for TWI. In addition, we apply the k -TWI (Algorithm 2) with three cut-off points ($n_1 \in \{0.25n, 0.5n, 0.75n\}$) to the simulated data. For the initializations of TWI, both linear interpolation and Kalman smoothing are used in our experiments. Kalman smoothing and the deterministic smoothing techniques are implemented via the `imputeTS` package (Moritz and Bartz-Beielstein, 2017) in R. The scalar filter algorithm (denoted as ScalarF henceforth) utilizes intervention analysis, and can be applied to multivariate and nonstationary series. Its implementation details are documented in Section S2 of the supplementary material.

5.1 Linear and nonlinear univariate time series

In this subsection, we consider the following data-generating processes (DGPs) for univariate time series, which can exhibit linear or nonlinear dynamic patterns. In the sequel, $\{\epsilon_t\}$ and $\{\epsilon_{t,j}\}$ for $j = 1, 2, \dots$ denote i.i.d. sequences of standard Gaussian variables.

DGP 1 (AR). $x_t = \phi x_{t-1} + \epsilon_t$, where ϕ is set to 0.8.

DGP 2 (ARMA). $(1 - \phi_1 B)x_t = (1 + \phi_2 B)\epsilon_t$, where B is the backshift operator and $(\phi_1, \phi_2) = (0.8, -0.6)$.

DGP 3 (TAR; Tong, 1983).

$$x_t = \begin{cases} \phi_1 x_{t-1} + \epsilon_t, & x_{t-1} \leq \tau \\ \phi_2 x_{t-1} + 0.5\epsilon_t, & x_{t-1} > \tau \end{cases},$$

where $(\phi_1, \phi_2, \tau) = (-2, 0.7, 1)$

DGP 4 (I(1) process). Data $\{x_t\}$ are generated according to $x_t = x_{t-1} + z_t + \epsilon_{t,2}$, where $z_t = \phi z_{t-1} + 0.5\epsilon_{t,1}$ with $\phi = -0.7$.

DGP 5 (Cyclic series with noise (CYC)). $x_t = 10 \cos(t(0.23\pi)) + 6 \cos(t(0.17\pi)) + 0.5\epsilon_t$.

DGPs 1 and 2 are well-known linear time series models. Note that DGP 2 admits an $\text{AR}(\infty)$ representation, so any finite-dimensional marginal distribution is inadequate to fully characterize the distribution of the underlying process. DGP 3 is a celebrated threshold AR model which has found many applications in modeling nonlinear dynamics in the econometrics and statistics literature (Montgomery et al., 1998; Li and Ling, 2012; Tsay and Chen, 2018). DGP 4 generates an $I(1)$ series which typically produces a highly persistent stochastic trend. Finally, DGP 5 features a deterministic cyclic trend with non-standard periods. Specifically, it includes two sinusoidal components with periods of 8.70 and 11.77, respectively.

Three measures of performance are considered. First, we report the Wasserstein distance (of order 2) between the empirical 3-dimensional marginal distributions of the imputed series and the full data. Specifically, let $\{\hat{w}_t^{(i)}\}$ and $\{x_t^{(i)}\}$ be the imputed series and the original series in simulation i , respectively, for $i = 1, 2, \dots, 1000$. We report

$$\frac{1}{1000} \sum_{i=1}^{1000} \mathcal{W}_2 \left(\frac{1}{n-3} \sum_{t=2}^{n-1} \delta_{(\hat{w}_t^{(i)}, \hat{w}_{t-1}^{(i)}, \hat{w}_{t-2}^{(i)})}, \frac{1}{n-3} \sum_{t=2}^{n-1} \delta_{(x_t^{(i)}, x_{t-1}^{(i)}, x_{t-2}^{(i)})} \right), \quad (14)$$

as a measure of how well the imputed series approximates the original series. Second, for DGP 1–4, the model parameters are estimated using the imputed series, and their root mean square errors (RMSEs) are reported. Third, we compare the RMSEs of the estimated autocovariance functions (ACFs). However, due to space constraints, we relegate the comparison of ACFs to Section S3.1 in the supplementary material.

The Wasserstein distance between the imputed and the original marginal distributions is reported in Table 1. Across all five DGPs employed, the smallest loss is consistently achieved by TWI-type methods, indicating that TWI effectively approximates the distributional properties of the underlying series. While other methods may yield good imputations for some specific DGPs, the result is not consistent across all processes. For instance, linear and spline interpolations show low Wasserstein loss for DGP 1, but their performance

is less competitive when applied to other models. In contrast, TWI methods, carefully initialized, consistently deliver solid performance across models and missing patterns. For the nonstationary Model 4 (I(1)), we first obtain an imputation $\{\hat{w}_t\}$ and consider the differenced series $\nabla \hat{w}_t = \hat{w}_t - \hat{w}_{t-1}$. Table 1 shows the Wasserstein distance between the marginal distributions implied by $\{\nabla \hat{w}_t\}$ and $\{\nabla x_t\}$. In this case, TWI consistently yields the lowest Wasserstein loss and greatly improves from its initialization.

Table 1 also shows TWI typically improves the Wasserstein loss from its initialization, often significantly. For example, for DGP 3 (TAR), TWI reduces the Wasserstein loss from Kalman smoothing initialization by approximately 45% under missing pattern I (from 1.38 to 0.74). Similarly, for DGP 5 (CYC), TWI reduces the Wasserstein loss by more than 50% from linear initialization (from 1.96 to 0.79). Figure 2 plots \hat{w}_t against \hat{w}_{t-1} when either or both are imputed under DGP 3, alongside (x_t, x_{t-1}) of the original data. While Kalman smoothing introduces substantial distortion in the marginal distribution, TWI, initialized by Kalman smoothing, significantly corrects this bias, producing imputations that capture the nonlinearity in the ground truth. Note that Kalman smoothing is done via an ARIMA state-space representation; hence the model is misspecified if the underlying process is nonlinear. Nevertheless, it already serves as a good initialization of TWI.

Next, we turn to the model parameters estimated from the imputed series. Table 2 presents the RMSEs for each model parameter. For DGP 1 (AR) and DGP 2 (ARMA), Kalman smoothing and the scalar filter yield satisfactory estimates among the benchmarks, with TWI offering only limited improvements. For the nonlinear DGP 3 (TAR), the results are drastically different. TWI produces the most accurate parameter estimates and can achieve more than 50% reduction in estimation errors compared to linear interpolation and Kalman smoothing. These estimation results demonstrate TWI’s strength in learning the underlying nonlinear dynamics. For DGP 4 (I(1)), TWI either outperforms or stays on par with the best benchmark, with Kalman filter being a strong initialization.

Table 1: Wasserstein distance between the empirical marginal distributions of the imputed series and those of the full data, averaged over 1000 simulations. TWI_{lin} denotes temporal Wasserstein imputation using linear interpolation as initialization and TWI_{Kal} denotes temporal Wasserstein imputation with Kalman smoothing as initialization. Similar notations are used for k -TWI. For DGP 4 (I(1)), the loss is computed using the first-differenced series. The smallest value for each model and missing pattern is marked in boldface.

Model	Linear	Spline	Kalman	ScalarF	TWI_{lin}	$k\text{-TWI}_{\text{lin}}$	TWI_{Kal}	$k\text{-TWI}_{\text{Kal}}$
Missing pattern I								
AR	0.41	0.41	0.42	0.50	0.40	0.44	0.41	0.44
ARMA	0.48	0.58	0.47	0.48	0.40	0.38	0.40	0.38
TAR	1.12	1.51	1.38	1.13	0.96	0.81	0.74	0.63
I(1)	0.71	0.75	0.62	4.38	0.58	0.53	0.54	0.50
CYC	1.96	0.82	0.77	1.97	0.79	0.77	0.60	0.70
NLVAR	2.98	3.42	3.01	2.94	2.25	2.14	2.19	2.12
AL ($\times 10$)	0.70	1.00	4.17	0.55	0.43	0.37	0.38	0.35
Missing pattern II								
AR	0.44	0.59	0.50	0.76	0.39	0.44	0.43	0.45
ARMA	0.47	1.29	0.51	0.53	0.36	0.34	0.40	0.35
TAR	1.04	3.11	1.25	0.99	0.84	0.73	0.76	0.61
I(1)	0.67	0.65	0.60	8.35	0.51	0.45	0.49	0.44
CYC	2.58	1.81	0.77	3.79	2.62	1.60	0.62	0.72
NLVAR	3.00	6.07	3.33	3.67	2.13	2.02	2.31	2.04
AL ($\times 10$)	0.56	1.83	3.81	0.46	0.36	0.33	0.40	0.34

5.2 Multivariate time series

In this subsection, we consider multivariate nonlinear time series models.

DGP 6 (Nonlinear VAR; NLVAR).

$$x_{t,1} = \phi_{11}x_{t-1,1} + \phi_{12}\mathfrak{s}(3x_{t-1,2}) + 0.25\epsilon_{t,1} \quad x_{t,2} = \phi_{21}x_{t-1,1} + \phi_{22}x_{t-1,2} + 3\epsilon_{t,2}$$

where $\mathfrak{s}(z) = 1/(1+\exp(-z))-0.5$ is the centered sigmoid function, and $(\phi_{11}, \phi_{12}, \phi_{21}, \phi_{22}) = (0.3, 8, 0, 0.4)$.

DGP 6 is a VAR model with a nonlinear term. In particular, the impact of $x_{t-1,2}$ on $x_{t,1}$ is nonlinear and is modeled by a sigmoid function. As depicted in Figure 3, TWI successfully captures the underlying nonlinear dynamics, whereas other imputation methods fail to preserve meaningful relationships. This is validated by the results shown in Table 1, where

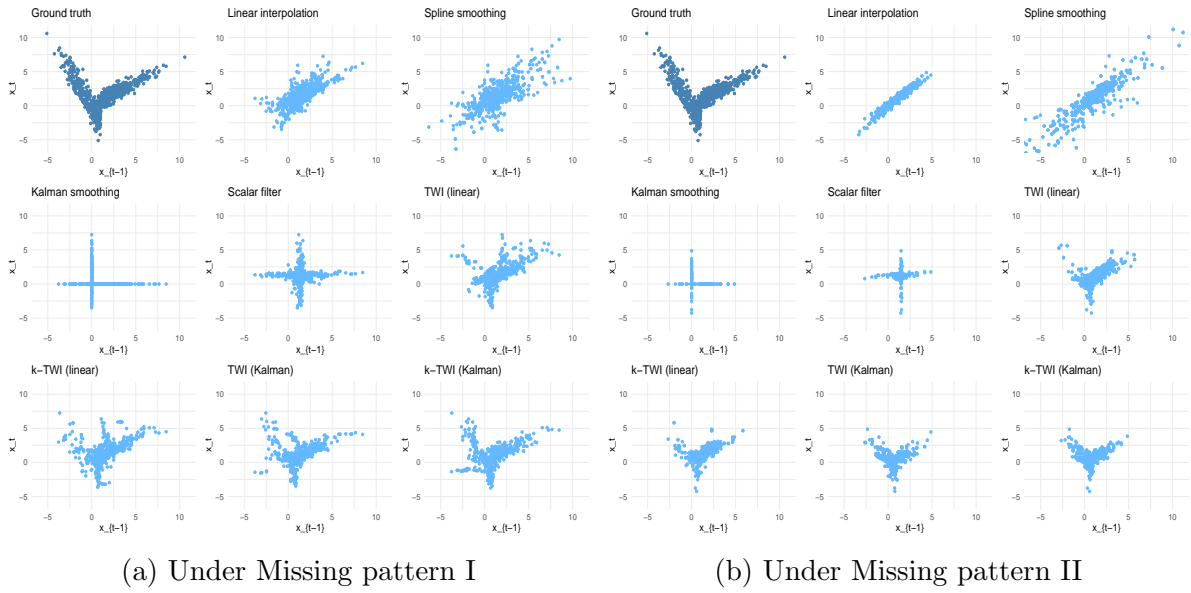


Figure 2: Scatter plot of (x_{t-1}, x_t) of the original data and $(\hat{w}_{t-1}, \hat{w}_t)$ of the imputed series, when the data are generated from Model 3 (TAR).

TWI achieves the lowest Wasserstein distance. Next, we assess the effectiveness of the imputed series in estimating the model parameters $(\phi_{11}, \phi_{12}, \phi_{21}, \phi_{22})$, assuming the nonlinear functional form is known. The root mean square estimation errors are documented in Table 2. Compared to the benchmarks, TWI provides considerable error reduction in the parameter associated with the nonlinear effect, ϕ_{12} . It attains more than 50% reduction in RMSE compared to the scalar filter, the best-performing benchmark.

We also consider a challenging multivariate nonlinear model, which generates the so-called compositional time series. The data are generated from the additive logistic (AL) model of [Brunsdon and Smith \(1998\)](#). Due to space constraints, we present its simulation results and discussion in Section S3.2 of the supplementary material.

6 Groundwater data application

In this section, we apply the proposed TWI to a groundwater dataset from Taiwan, which was collected and analyzed by [Hsu et al. \(2020\)](#). Given the island’s steep topography and varying rainfall distribution, groundwater management is of considerable importance for

Table 2: Estimation root mean square errors for parameter estimation errors. The results are averaged over 1000 simulations. See Table 1 for notations.

Model		Linear	Spline	Kalman	ScalarF	TWI _{lin}	k -TWI _{lin}	TWI _{Kal}	k -TWI _{Kal}
Missing pattern I									
AR	ϕ	0.06	0.06	0.05	0.03	0.03	0.04	0.03	0.04
ARMA	ϕ_1	0.19	0.47	0.12	0.08	0.17	0.16	0.11	0.11
	ϕ_2	0.46	0.95	0.18	0.10	0.33	0.26	0.16	0.15
TAR	ϕ_1	1.02	1.67	0.82	0.63	0.71	0.58	0.53	0.44
	ϕ_2	0.08	0.07	0.20	0.04	0.05	0.03	0.03	0.02
	τ	0.01	0.75	0.35	0.20	0.05	0.05	0.03	0.03
I(1)	ϕ	0.96	0.47	0.45	0.68	0.48	0.32	0.30	0.24
NLVAR	ϕ_{11}	0.19	0.27	0.15	0.03	0.06	0.03	0.05	0.03
	ϕ_{12}	3.10	3.16	2.87	1.67	1.34	1.02	1.22	0.97
	ϕ_{21}	0.03	0.07	0.03	0.03	0.03	0.03	0.03	0.03
	ϕ_{21}	0.18	0.23	0.10	0.04	0.05	0.04	0.04	0.04
Missing pattern II									
AR	ϕ	0.05	0.07	0.04	0.04	0.03	0.02	0.03	0.02
ARMA	ϕ_1	0.04	0.08	0.09	0.08	0.05	0.06	0.09	0.09
	ϕ_2	0.16	0.61	0.11	0.10	0.12	0.11	0.11	0.12
TAR	ϕ_1	0.72	2.44	0.38	0.25	0.25	0.20	0.29	0.21
	ϕ_2	0.09	0.12	0.05	0.03	0.06	0.05	0.02	0.01
	τ	0.01	1.72	0.01	0.01	0.01	0.01	0.01	0.01
I(1)	ϕ	0.08	1.08	0.11	0.70	0.09	0.10	0.10	0.10
NLVAR	ϕ_{11}	0.19	0.44	0.08	0.02	0.02	0.01	0.02	0.01
	ϕ_{12}	2.67	3.51	1.68	1.26	0.61	0.46	0.61	0.43
	ϕ_{21}	0.02	0.09	0.03	0.03	0.06	0.05	0.04	0.03
	ϕ_{21}	0.15	0.34	0.05	0.04	0.04	0.04	0.04	0.04

Taiwan, particularly as it is a critical water source. However, the statistical analysis of groundwater levels is challenged by frequent missing data, especially from deeper wells.

We aim to study the seasonal groundwater variations, for which we first transform the hourly data from 352 sites between October 1992 and August 2020 into monthly records. For each site, monthly groundwater level is calculated as the average of the observations in a given month, with months classified as missing if more than one-third of the observations are missing. Our analysis focuses on sites with a less-than-median amount of missing data, reducing the sample to 176 sites. Figure 4 shows the monthly groundwater levels for these



Figure 3: Scatter plots of $(x_{t-1,i}, x_{t,j})$ of the original data and $(\hat{w}_{t-1,i}, \hat{w}_{t,j})$ of the imputed series for $i, j \in \{1, 2\}$, when the data are generated from Model 6 under missing pattern II.

sites, after subtracting the mean and normalizing by the standard deviation. We make two observations. First, many series exhibit strong seasonality due to the rainfall pattern in Taiwan. Monsoon and typhoons increase rainfall in summer, while winters are drier. Second, there are many outlying values and anomalies in the observed series, including

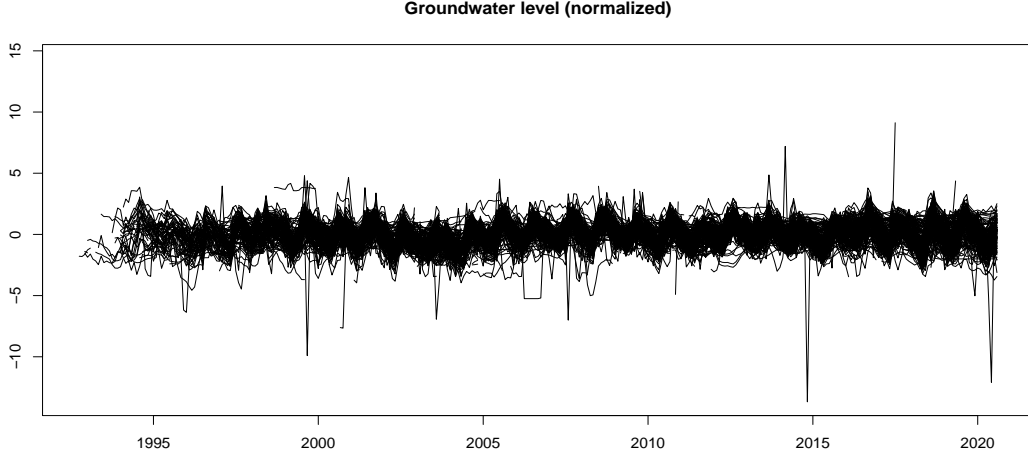


Figure 4: Time plot of the groundwater levels of the 176 sites under study. Each series is normalized by subtracting its mean and dividing by its standard deviation.

abrupt changes in groundwater levels that are more than 5 standard deviations from the sample mean. We also treat such extreme values as missing data.

During the period from October, 1992 to August, 2020, few months recorded valid observations at all sites. Figure 5 shows the fluctuations in the percentage of sites with missing data over time. Although missing data are mostly prevalent in the early years, there are some time during which the percentage surges, such as between 2003 and 2005. In addition, the percentage is gradually increasing in more recent years. Thus, one may lose much information if the analysis is restricted to sites with relatively complete records.

We consider two downstream tasks using the imputed series. First, following [Hsu et al. \(2020\)](#), we decompose the de-trended time series using the independent component analysis (ICA), for which we apply the fastICA algorithm of [Hyvärinen and Oja \(2000\)](#). Because direct application of ICA becomes infeasible when the series are severely corrupted by missing data, the analysis of [Hsu et al. \(2020\)](#) is confined to a relatively short time span. The second downstream task considers autoregressive modeling, which is presented in Section S3.3 in the supplementary material. In implementation, we chose $n_1 = 160$ and $p = 6$ for

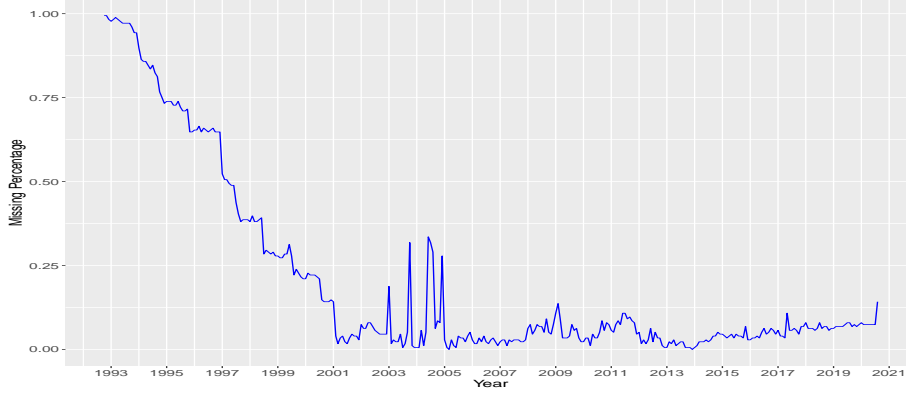


Figure 5: Monthly percentage of sites recording a missing value.

TWI, and for k -TWI we use $n_1 \in \{160, 225, 110\}$.

Figure 6 shows the leading two independent components (ICs) estimated using the imputed series. ICs estimated from series imputed by Kalman smoothing have peaks around August-September (red shaded area) and May-June (blue shaded area), which was also observed in Hsu et al. (2020). These peaks are attributed to the dual rain seasons in Taiwan, which involve typhoons in August-September and the Meiyu period from mid-May to mid-June. ICs estimated from TWI-imputed series with Kalman initialization largely preserve these seasonal peaks, but with improved performance before 2002. Recall that missing data are prevalent during this period (Figure 5). Especially for the first IC, those computed from TWI-imputed series have clear peaks around August-September with a more consistent amplitude. On the other hand, the ICs computed from the linearly interpolated series could not effectively isolate and identify the Meiyu season, with peaks occurring slightly earlier than expected. Nonetheless, ICs estimated from TWI-imputed series with linear interpolation substantially alleviates this shortcoming and produced more interpretable results. ICs computed from spline-interpolated series also identifies the two rain seasons, albeit they show more rugged trajectories instead of clean periodic patterns. For the scalar filter, the resulting ICs similarly appear noisy, and the Meiyu season is not well-isolated, showing that the imputation induces distortions in the dynamic pattern.

Overall, TWI took a more holistic view which accounts for the underlying dynamics,

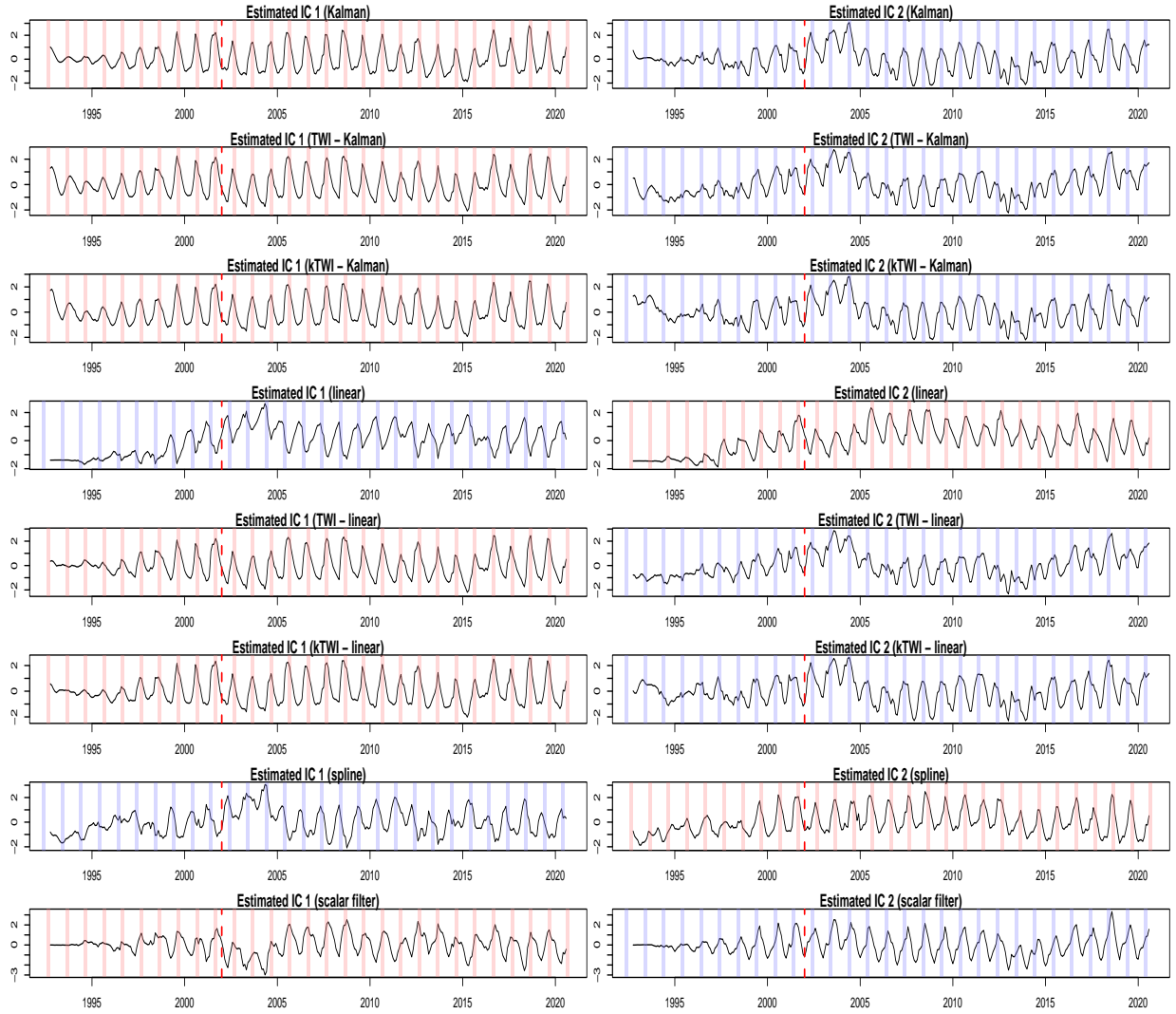


Figure 6: Independent components estimated using the imputed series. The dashed red lines in each plot mark January 2002. The red and blue shaded areas correspond to August-September (typhoon season) and May-June (Meiyu season), respectively.

such as complex seasonality, and produced interpretable results. In Section S3.3 of the supplementary material, we conduct further experiments to show that the marginal distributions of TWI-imputed series, in terms of AR modeling, are also more consistent across time compared to other methods. These results show TWI performs reliably in practice and is a useful method in handling missing data in time series.

SUPPLEMENTARY MATERIAL

Supplementary material: The file contains the proofs of the propositions presented in

Section 4 and some technical results. It also documents the scalar filter algorithm of Peña and Tsay (2021) and complementary numerical results, including the simulation results for autocovariance estimation and for data generated from a compositional time series model. Finally, it includes the analysis of the groundwater data via autoregressive modeling.

References

- Alonso, A. M. and Sipols, A. E. (2008). A time series bootstrap procedure for interpolation intervals. *Computational Statistics & Data Analysis*, 52(4):1792–1805.
- Billingsley, P. (1995). *Probability and Measure*. Wiley Series in Probability and Statistics. Wiley.
- Boyd, S. and Vandenberghe, L. (2004). *Convex Optimization*. Cambridge University Press.
- Brenier, Y. (1987). Décomposition polaire et réarrangement monotone des champs de vecteurs. *CR Acad. Sci. Paris Sér. I Math.*, 305:805–808.
- Brunsdon, T. M. and Smith, T. (1998). The time series analysis of compositional data. *Journal of Official Statistics*, 14(3):237–253.
- Carrizosa, E., Olivares-Nadal, A. V., and Ramírez-Cobo, P. (2013). Time series interpolation via global optimization of moments fitting. *European Journal of Operational Research*, 230(1):97–112.
- Cuturi, M. (2013). Sinkhorn distances: Lightspeed computation of optimal transport. In *Advances in Neural Information Processing Systems*, volume 26.
- Galichon, A. (2016). *Optimal Transport Methods in Economics*. Princeton University Press.

- Gómez, V., Maravall, A., and Peña, D. (1999). Missing observations in arima models: Skipping approach versus additive outlier approach. *Journal of Econometrics*, 88(2):341–363.
- Grippo, L. and Sciandrone, M. (2000). On the convergence of the block nonlinear gauss–seidel method under convex constraints. *Operations Research Letters*, 26(3):127–136.
- Harvey, A., Hurn, S., Palumbo, D., and Thiele, S. (2024). Modelling circular time series. *Journal of Econometrics*, 239(1):105450.
- Harvey, A. C. and Pierse, R. G. (1984). Estimating missing observations in economic time series. *Journal of the American Statistical Association*, 79(385):125–131.
- Hastie, T., Tibshirani, R., and Friedman, J. (2009). *The Elements of Statistical Learning: Data Mining, Inference, and Prediction*. Springer series in statistics. Springer New York, NY.
- Hsu, Y.-J., Fu, Y., Bürgmann, R., Hsu, S.-Y., Lin, C.-C., Tang, C.-H., and Wu, Y.-M. (2020). Assessing seasonal and interannual water storage variations in taiwan using geodetic and hydrological data. *Earth and Planetary Science Letters*, 550:116532.
- Hyvärinen, A. and Oja, E. (2000). Independent component analysis: algorithms and applications. *Neural Networks*, 13(4):411–430.
- Li, D. and Ling, S. (2012). On the least squares estimation of multiple-regime threshold autoregressive models. *Journal of Econometrics*, 167(1):240–253.
- Little, R. and Rubin, D. (2019). *Statistical Analysis with Missing Data*. Wiley Series in Probability and Statistics. Wiley.
- McElroy, T. (2022). Casting vector time series: algorithms for forecasting, imputation, and signal extraction. *Electronic Journal of Statistics*, 16(2):5534–5569.

- McElroy, T. and Politis, D. (2020). *Time series: A first course with bootstrap starter*. Chapman and Hall.
- McElroy, T. S. and Politis, D. N. (2022). Optimal linear interpolation of multiple missing values. *Statistical Inference for Stochastic Processes*, 25(3):471–483.
- Montgomery, A. L., Zarnowitz, V., Tsay, R. S., and Tiao, G. C. (1998). Forecasting the u.s. unemployment rate. *Journal of the American Statistical Association*, 93(442):478–493.
- Moritz, S. and Bartz-Beielstein, T. (2017). imputeTS: Time series missing value imputation in r. *The R Journal*, 9(1):207–218.
- Parikh, N., Boyd, S., et al. (2014). Proximal algorithms. *Foundations and trends[®] in Optimization*, 1(3):127–239.
- Peña, D. and Maravall, A. (1991). Interpolation, outliers and inverse autocorrelations. *Communications in Statistics - Theory and Methods*, 20(10):3175–3186.
- Peña, D., Tiao, G., and Tsay, R. (2011). *A Course in Time Series Analysis*. Wiley Series in Probability and Statistics. Wiley.
- Peña, D. and Tsay, R. (2021). *Statistical Learning for Big Dependent Data*. Wiley Series in Probability and Statistics. Wiley.
- Peyré, G. and Cuturi, M. (2019). *Computational Optimal Transport: With Applications to Data Science*. Foundations and trends in machine learning. Now Publishers.
- Pourahmadi, M. (1989). Estimation and interpolation of missing values of a stationary time series. *Journal of Time Series Analysis*, 10(2):149–169.
- Tong, H. (1983). *Threshold Models in Nonlinear Time Series Analysis*. Lecture Notes in Statistics. Springer New York, NY.

- Tsay, R. and Chen, R. (2018). *Nonlinear Time Series Analysis*. Wiley Series in Probability and Statistics. Wiley.
- Villani, C. (2008). *Optimal Transport: Old and New*. Grundlehren der mathematischen Wissenschaften. Springer Berlin, Heidelberg.
- Villani, C. (2021). *Topics in Optimal Transportation*. Graduate Studies in Mathematics. American Mathematical Society.
- Zheng, T. and Chen, R. (2017). Dirichlet arma models for compositional time series. *Journal of Multivariate Analysis*, 158:31–46.
- Zhu, C. and Müller, H.-G. (2024). Spherical autoregressive models, with application to distributional and compositional time series. *Journal of Econometrics*, 239(2):105389.

Supplementary material to “Temporal Wasserstein Imputation: Versatile Missing Data Imputation for Time Series”

This supplementary material contains three sections. Section S1 collects the proofs of the propositions presented in main text as well as some technical results. Section S2 documents the scalar filter algorithm of [Peña and Tsay \(2021\)](#) for completeness. Section S3 contains complementary numerical results, including the simulation results for autocovariance estimation and imputing data generated from a compositional time series model. It also includes the analysis of autoregressive modeling using the imputed groundwater data.

S1 Technical proofs

Proof of Proposition 3. Clearly, (a) holds by construction of the algorithm. Since Algorithm 1 is an instance of the Gauss-Siedel algorithm, (b) follows from [Grippo and Scian-drone \(2000\)](#). Thus it remains to prove (c). Optimizing $\mathbf{\Pi}$ while holding \mathbf{w} fixed is the optimal transport problem, which is clearly convex. Now fix $\mathbf{\Pi}$. Note that

$$\begin{aligned} F(\mathbf{w}, \mathbf{\Pi}) &= \sum_{i=p-1}^{n_1} \sum_{j=n_1+1}^{n-1} \pi_{ij} \sum_{h=0}^{p-1} \ell(w_{i-h} - w_{j-h}) + \frac{\lambda}{2} \|\mathbf{w}\|^2 \\ &= \sum_{h=0}^{p-1} \underbrace{\sum_{i=p-1}^{n_1} \sum_{j=n_1+1}^{n-1} \pi_{ij} \ell(w_{i-h} - w_{j-h})}_{F_h(\mathbf{w}, \mathbf{\Pi})} + \frac{\lambda}{2} \|\mathbf{w}\|^2. \end{aligned}$$

It suffices to show each F_h is convex in \mathbf{w} . In the following, we only prove the case of F_0 since the arguments for the other cases are similar. Let $\mathbf{u} = (w_{p-1}, w_1, \dots, w_{n_1})^\top$ and $\mathbf{v} = (w_{n_1+1}, \dots, w_{n-1})^\top$. Then

$$\begin{aligned} \frac{\partial F_0}{\partial \mathbf{u}} &= \left(\sum_{j=n_1+1}^{n-1} \pi_{ij} \ell'(w_i - w_j) : i = p-1, \dots, n_1 \right)^\top, \\ \frac{\partial F_0}{\partial \mathbf{v}} &= \left(- \sum_{i=p-1}^{n_1} \pi_{ij} \ell'(w_i - w_j) : j = n_1+1, \dots, n-1 \right)^\top. \end{aligned}$$

Moreover,

$$\frac{\partial^2 F_0}{\partial \mathbf{u}^2} = \text{diag} \left(\sum_{j=n_1+1}^{n-1} \pi_{ij} \ell''(w_i - w_j) : i = p-1, \dots, n_1 \right), \quad (\text{S1.1})$$

$$\frac{\partial^2 F_0}{\partial \mathbf{v}^2} = \text{diag} \left(\sum_{i=p-1}^{n_1} \pi_{ij} \ell''(w_i - w_j) : j = n_1+1, \dots, n-1 \right), \quad (\text{S1.2})$$

$$\frac{\partial^2 F_0}{\partial \mathbf{u} \partial \mathbf{v}} = -(\pi_{ij} \ell''(w_i - w_j))_{p-1 \leq i \leq n_1, n_1+1 \leq j \leq n-1}. \quad (\text{S1.3})$$

Since ℓ is convex, $\ell'' \geq 0$. From (S1.1)–(S1.3), it is readily seen that the Hessian matrix $\mathbf{H} = \partial^2 F_0 / \partial \mathbf{w}^2$ is weakly diagonally dominant with nonnegative diagonal entries. It follows from the Gershgorin circle theorem that \mathbf{H} is positive semi-definite. Thus F_0 is convex in \mathbf{w} . \square

Before proving Proposition 4, we first state our assumptions and establish Lemma S6.

(A1) The underlying time series $\{\tilde{x}_t\}$ is stationary and ergodic.

(A2) $\mathbb{E}|\tilde{x}_t|^k < \infty$ for some $k \geq 1$.

These assumptions are satisfied by many linear and nonlinear time series models.

Lemma S6. *Suppose $\{\tilde{x}_t\}$ satisfies (A1) and (A2). Then*

$$\mathcal{W}_k \left(\frac{1}{n-p+1} \sum_{t=p-1}^{n-1} \delta_{\mathbf{v}_t(\tilde{\mathbf{x}})}, \mu_p \right) \xrightarrow{n \rightarrow \infty} 0 \quad \text{a.s.},$$

where $\tilde{\mathbf{x}} = (\tilde{x}_0, \dots, \tilde{x}_{n-1})$.

Proof. By Theorem 7.12 of Villani (2021), it suffices to show that with probability one,

$$\frac{1}{n-p+1} \sum_{t=p-1}^{n-1} \delta_{\mathbf{v}_t(\tilde{\mathbf{x}})} \Rightarrow \mu_p, \quad (\text{S1.4})$$

and

$$\frac{1}{n-p+1} \sum_{t=p-1}^{n-1} \|\mathbf{v}_t(\tilde{\mathbf{x}})\|^k \rightarrow \mathbb{E} \|\mathbf{v}_{p-1}(\tilde{\mathbf{x}})\|^k. \quad (\text{S1.5})$$

By Theorem 36.4 of Billingsley (1995), the processes $\{\|\mathbf{v}_t(\tilde{\mathbf{x}})\|^k\}_t$ and $\{\exp(i\mathbf{h}^\top \mathbf{v}_t(\tilde{\mathbf{x}}))\}_t$ are stationary and ergodic for any $\mathbf{h} \in \mathbb{R}^p$, where $i = \sqrt{-1}$. Thus (S1.5) follows immediately from the Ergodic theorem. To show (S1.4), it suffices to show, with probability one,

$$\hat{\varphi}_n(\mathbf{h}) := \frac{1}{n-p+1} \sum_{t=p-1}^{n-1} \exp(i\mathbf{h}^\top \mathbf{v}_t(\tilde{\mathbf{x}})) \rightarrow \int \exp(i\mathbf{h}^\top \mathbf{v}) d\mu_p(\mathbf{v}) =: \varphi(\mathbf{h}) \quad \text{for all } \mathbf{h} \in \mathbb{R}^p.$$

By the Ergodic theorem, we have

$$\hat{\varphi}_n(\mathbf{q}) \rightarrow \varphi(\mathbf{q}), \quad \text{for all } \mathbf{q} \in \mathbb{Q}^p, \quad (\text{S1.6})$$

with probability one. Let

$$\mathcal{E} = \{\hat{\varphi}_n(\mathbf{q}) \rightarrow \varphi(\mathbf{q}) \text{ for all } \mathbf{q} \in \mathbb{Q}^p\} \cap \left\{ \frac{1}{n-p+1} \sum_{t=p-1}^{n-1} \|\mathbf{v}_t(\tilde{\mathbf{x}})\| \rightarrow \mathbb{E}\|\mathbf{v}_{p-1}(\tilde{\mathbf{x}})\| \right\},$$

noting that $\mathbb{E}\|\mathbf{v}_{p-1}(\tilde{\mathbf{x}})\| < \infty$ by (A2). By the Ergodic theorem and (S1.6), $\mathbb{P}(\mathcal{E}) = 1$. Fix $\omega \in \mathcal{E}$ and let $\epsilon > 0$ and $\mathbf{h} \in \mathbb{R}^p$ be arbitrary. Since φ is uniformly continuous, there exists $\delta > 0$ such that

$$|\varphi(\mathbf{h}) - \varphi(\mathbf{q})| < \epsilon, \quad (\text{S1.7})$$

for all $\mathbf{q} \in \mathbb{Q}^p$ with $\|\mathbf{h} - \mathbf{q}\| < \delta$. In addition, using $|\exp(i\mathbf{h}^\top \mathbf{z}) - 1| \leq \|\mathbf{h}\| \|\mathbf{z}\|$, we have

$$|\hat{\varphi}_n(\mathbf{h}) - \hat{\varphi}_n(\mathbf{q})| \leq \frac{\delta}{n-p+1} \sum_{t=p-1}^{n-1} \|\mathbf{v}_t(\tilde{\mathbf{x}})\|, \quad (\text{S1.8})$$

for all \mathbf{h}, \mathbf{q} such that $\|\mathbf{h} - \mathbf{q}\| < \delta$. Combining (S1.7)–(S1.8), we have

$$\begin{aligned} |\hat{\varphi}_n(\mathbf{h}) - \varphi(\mathbf{h})| &\leq |\hat{\varphi}_n(\mathbf{h}) - \hat{\varphi}_n(\mathbf{q})| + |\hat{\varphi}_n(\mathbf{q}) - \varphi(\mathbf{q})| + |\varphi(\mathbf{q}) - \varphi(\mathbf{h})| \\ &\leq \frac{\delta}{n-p+1} \sum_{t=p-1}^{n-1} \|\mathbf{v}_t(\tilde{\mathbf{x}})\| + o(1) + \epsilon \end{aligned}$$

on $\omega \in \mathcal{E}$. Note, in particular, that ϵ and δ do not depend on \mathbf{h} . Letting $\epsilon \rightarrow 0$ and $\delta \rightarrow 0$ proves (S1.4) holds on \mathcal{E} , and hence with probability one. \square

Proof of Proposition 4. We only consider the case $\mathcal{M}_n \subseteq \{n_1 + 1, \dots, n - 1\}$ here as the other case follows from a similar argument. Define

$$\begin{aligned}\hat{\mu}_{\text{pre}} &:= \frac{1}{n_1 - p + 2} \sum_{t=p-1}^{n_1} \delta_{\mathbf{v}_t(\hat{\mathbf{w}})} = \frac{1}{n_1 - p + 2} \sum_{t=p-1}^{n_1} \delta_{\mathbf{v}_t(\bar{\mathbf{x}})} =: \mu_{\text{pre}}, \\ \hat{\mu}_{\text{post}} &:= \frac{1}{n - n_1 - 1} \sum_{t=n_1+1}^{n-1} \delta_{\mathbf{v}_t(\hat{\mathbf{w}})} \\ \mu_{\text{post}} &:= \frac{1}{n - n_1 - 1} \sum_{t=n_1+1}^{n-1} \delta_{\mathbf{v}_t(\bar{\mathbf{x}})}\end{aligned}$$

Since the Wasserstein distance of order k is a metric on the space of probability measures with finite k -th moments, we have

$$\begin{aligned}\mathcal{W}_k(\hat{\mu}_{\text{post}}, \mu_p) &\leq \mathcal{W}_k(\hat{\mu}_{\text{post}}, \hat{\mu}_{\text{pre}}) + \mathcal{W}_k(\mu_{\text{pre}}, \mu_p) \\ &\leq \mathcal{W}_k(\mu_{\text{post}}, \mu_{\text{pre}}) + \mathcal{W}_k(\mu_{\text{pre}}, \mu_p) \\ &\leq \mathcal{W}_k(\mu_{\text{post}}, \mu_p) + 2\mathcal{W}_k(\mu_{\text{pre}}, \mu_p).\end{aligned}$$

Now the desired result follows from Lemma S6. □

S2 Scalar filter algorithm

The following summarizes the scalar filter algorithm of Peña and Tsay (2021).

- Initialize the imputation $\hat{\mathbf{w}}^{(0)} = (\hat{w}_0^{(0)}, \hat{w}_1^{(0)}, \dots, \hat{w}_{n-1}^{(0)})^\top$ with $\hat{w}_t^{(0)} = 0$ if $t \in \mathcal{M}$.
- For each $s \in \mathcal{M}$, let $I_t^{(s)}$ be the indicator function. That is,

$$I_t^{(s)} = \begin{cases} 1, & t = s \\ 0, & t \neq s \end{cases}$$

and estimate the intervention model using $\hat{\mathbf{w}}^{(0)}$. For example, one can fit an ARX model with $\{I_t^{(s)} : s \in \mathcal{M}\}$ as exogenous predictors.

- Let $\hat{\beta}^{(s)}$ be the intervention effect associated with $I_t^{(s)}$. Estimate the missing data by

$$\hat{w}_s = \hat{w}_s^{(0)} - \hat{\beta}^{(s)}, \quad s \in \mathcal{M}.$$

As one can see from the algorithm above, the scalar filter algorithm proposed by [Peña and Tsay \(2021\)](#) is based on intervention analysis. It can be iterated in order to improve the estimates. However, no convergence guarantee is provided by the authors.

When fitting an ARX model with the indicators as exogenous predictors, if there are many missing values, standard approaches may be infeasible or unreliable due to near collinearity. In this case, we employ a small ℓ_2 penalty to avoid numerical instability.

S3 Complementary numerical results

S3.1 Autocovariance estimation

In this subsection, we compare the ACFs estimated from the imputed series. Define $\gamma(\mathbf{z}, h) = (n-h)^{-1} \sum_{t=h}^{n-1} (z_t - \bar{z})(z_{t-h} - \bar{z})$, where $\mathbf{z} = (z_0, z_1, \dots, z_{n-1})$ and $\bar{z} = n^{-1} \sum_{t=0}^{n-1} z_t$. Then the RMSE is defined as

$$\text{RMSE}_\gamma(h) = \sqrt{\frac{1}{1000} \sum_{i=1}^{1000} (\gamma(\hat{\mathbf{w}}^{(i)}, h) - \gamma_{\mathbf{x}}(h))^2}, \quad (\text{S3.9})$$

where $\hat{\mathbf{w}}^{(i)} = (\hat{w}_0^{(i)}, \dots, \hat{w}_{n-1}^{(i)})$ and $\gamma_{\mathbf{x}}(h) = \frac{1}{1000} \sum_{i=1}^{1000} \gamma(\mathbf{x}^{(i)}, h)$ with $\mathbf{x}^{(i)} = (x_0^{(i)}, \dots, x_{n-1}^{(i)})$.

Table [S1](#) reports $\text{RMSE}_\gamma(h)$ for $h = 0, 1, 2$. For Model [1](#) (AR), most methods perform reasonably well. Linear interpolation produces accurate ACF estimates since the positive AR coefficient intrinsically favors linearity, while the scalar filter exhibits largest estimation errors. For Model [2](#) (ARMA), TWI improves from linear and Kalman initializations and yields more accurate ACF estimates: TWI reduces the biases in Kalman smoothing when $h = 0$ and in linear interpolation when $h = 1$, and $h = 2$. For the nonlinear Model [3](#) (TAR), the ACFs estimated from the TWI-imputed series exhibit the lowest RMSEs, with substantial improvements over the initializations. Notably, the scalar filter also yields accurate ACFs for $h = 1, 2$. Figure [S1](#) plots the histogram of the estimated ACFs at lag 1 (that is, $\gamma(\hat{\mathbf{w}}^{(i)}, 1)$), which shows how TWI effectively nullifies the biases caused by the initializations.

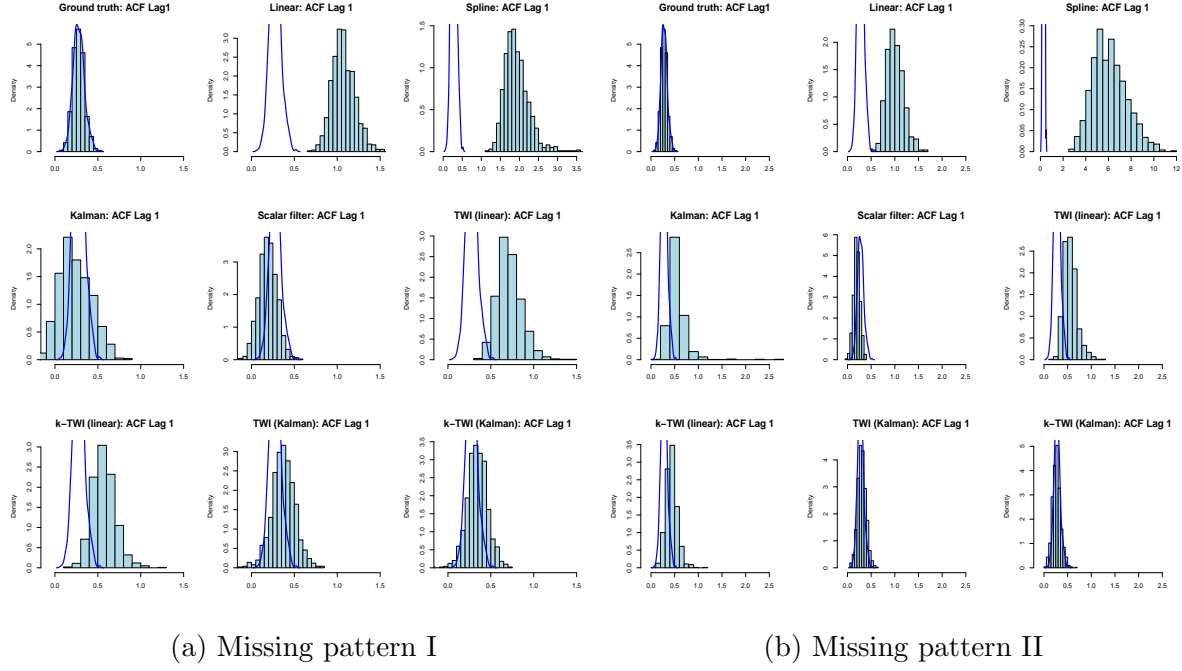


Figure S1: Histogram of estimated autocovariance function at lag 1 when the data are generated from Model 3 (TAR). The blue line is the smoothed density estimated from the histogram of the ACFs estimated from the ground truth.

The advantage of TWI becomes even more pronounced in nonstationary models 4 (I(1)) and 5 (CYC), for which it achieves low ACF estimation errors. The scalar filter performs poorly for these models, which is likely the consequence of using many indicators in the intervention analysis. Among the benchmarks, Kalman filter produces the best result for these two models, but it can be further improved by the proposed TWI procedure.

S3.2 Compositional time series

In this subsection, we discuss the simulation results associated with the following model.

DGP 7 (Additive logistic model; AL, [Brunsdon and Smith, 1998](#)).

$$y_{t,1} = 0.1 + 0.7y_{t-1,1} - 0.5y_{t-1,2} + 0.2\epsilon_{t,1}$$

$$y_{t,2} = 0.1 - 0.7y_{t-1,2} + 0.2\epsilon_{t,2}$$

Table S1: $\text{RMSE}_\gamma(h)$, defined in (S3.9), for $h = 0, 1, 2$, with h denoting lag. The results are averaged over 1000 simulations, and the smallest values in each row are marked in boldface. See Table 1 in the main text for notations.

Model	h	Linear	Spline	Kalman	ScalarF	TWI_{lin}	$k\text{-TWI}_{\text{lin}}$	TWI_{Kal}	$k\text{-TWI}_{\text{Kal}}$
Missing pattern I									
AR	0	0.32	0.29	0.37	0.50	0.30	0.31	0.32	0.32
	1	0.26	0.34	0.29	0.47	0.27	0.30	0.28	0.31
	2	0.26	0.27	0.29	0.38	0.25	0.28	0.27	0.29
ARMA	0	0.14	0.19	0.29	0.31	0.13	0.13	0.22	0.18
	1	0.22	0.44	0.07	0.08	0.14	0.10	0.07	0.07
	2	0.08	0.08	0.07	0.07	0.06	0.06	0.07	0.07
TAR	0	0.59	0.77	0.73	1.07	0.65	0.56	0.56	0.45
	1	0.81	1.68	0.19	0.14	0.46	0.32	0.17	0.13
	2	0.40	0.31	0.16	0.11	0.24	0.16	0.10	0.09
I(1)	0	0.52	0.40	0.48	19.41	0.42	0.35	0.40	0.34
	1	0.35	0.51	0.25	9.32	0.28	0.25	0.22	0.21
	2	0.17	0.35	0.11	1.28	0.15	0.14	0.11	0.11
CYC	0	10.94	2.40	3.90	4.67	1.81	1.25	0.68	0.62
	1	9.05	1.72	3.33	5.88	1.47	1.04	0.54	0.51
	2	1.90	0.46	0.81	2.13	0.41	0.33	0.17	0.18
Missing pattern II									
AR	0	0.38	0.70	0.55	0.78	0.33	0.36	0.43	0.39
	1	0.28	0.79	0.42	0.70	0.29	0.34	0.37	0.36
	2	0.26	0.66	0.36	0.65	0.27	0.31	0.34	0.34
ARMA	0	0.14	1.35	0.31	0.32	0.13	0.11	0.24	0.17
	1	0.17	1.49	0.08	0.09	0.10	0.08	0.07	0.07
	2	0.15	1.05	0.07	0.08	0.09	0.07	0.07	0.07
TAR	0	0.49	5.39	0.71	1.08	0.72	0.68	0.73	0.65
	1	0.75	6.04	0.34	0.11	0.31	0.20	0.09	0.09
	2	0.77	4.36	0.34	0.10	0.42	0.28	0.19	0.14
I(1)	0	0.47	0.27	0.47	51.84	0.38	0.30	0.36	0.29
	1	0.19	0.43	0.18	0.56	0.17	0.14	0.14	0.13
	2	0.08	0.08	0.07	0.52	0.08	0.08	0.07	0.07
CYC	0	7.46	7.56	1.96	15.21	12.27	6.49	1.26	1.03
	1	2.63	3.99	1.45	16.23	9.57	5.07	0.98	0.83
	2	11.18	5.09	0.79	7.90	1.28	1.04	0.28	0.31

and the observed data are

$$x_{t,j} = \begin{cases} \frac{\exp(y_{t,j})}{1 + \exp(y_{t,1}) + \exp(y_{t,2})}, & j = 1, 2, \\ \frac{1}{1 + \exp(y_{t,1}) + \exp(y_{t,2})}, & j = 3. \end{cases}$$

DGP 7 generates the so-called compositional time series, which refers to a multivariate time series $\mathbf{x}_t = (x_{t,1}, \dots, x_{t,d})^\top$, $d > 1$, such that for each t , $\sum_{j=1}^d x_{t,j} = 1$, and $x_{t,j} \geq 0$ for all j . Such data are encountered in a wide array of fields such as the environmental sciences, economics, geology and political science. Here, we adopt the additive logistic (AL) model of [Brunsdon and Smith \(1998\)](#) in DGP 7. The AL model postulates that after some nonlinear transformation, the data follow a standard VARMA model. Alternative models for composition time series include the recent works of [Zheng and Chen \(2017\)](#), [Harvey et al. \(2024\)](#), and [Zhu and Müller \(2024\)](#).

Table 1 in the main paper records the Wasserstein distance between the 3-dimensional marginal distributions of the imputed and original series. With the smallest Wasserstein loss, TWI methods again demonstrate their ability to adapt to nonlinear dependence structures. It is worth noting that while the linear interpolation results in a compositional series, other methods, such as the Kalman smoothing, do not generally maintain this compositional property. By restricting the admissible set, TWI ensures that the imputed series remain compositional. As shown in Figure S2, linear interpolation falsely promotes negative correlation between $\hat{w}_{t,3}$ and $\hat{w}_{t-1,2}$ and Kalman smoothing often deviates from the plausible range of a compositional series. TWI amends these peculiarities, leading to imputations that align more closely with the underlying data.

S3.3 Autoregressive modeling with groundwater data

As our second downstream task for the groundwater data analysis, we fit an AR(6) model using data imputed by the methods considered. The training data consists of the early period between October, 1992 and September, 2002, amounting to 120 data points per series, including imputed values. Then, we assess the impact of imputation quality by the out-of-sample prediction performance in predicting the remaining data. The missing data in the test data are removed for fair comparison. Figure S3 presents, in violin plots, the

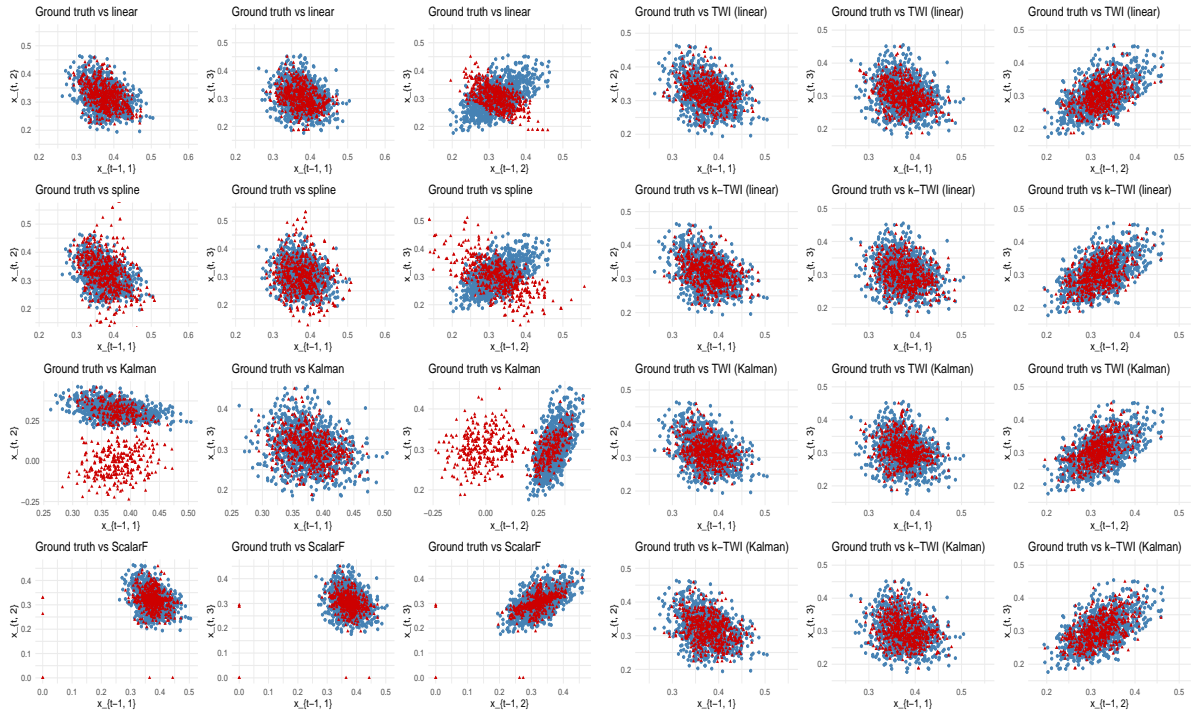


Figure S2: Scatter plots of $(x_{t-1,i}, x_{t,j})$ of the original data (plotted in blue) and $(\hat{w}_{t-1,i}, \hat{w}_{t,j})$ of the imputed series (plotted in red) for $i, j = 1, 2, 3, i \neq j$, when the data are generated from Model 7 (AL) under missing pattern I.

distribution of the logarithm of the root mean squared prediction errors (log RMSE) for each method across the 176 series under study. The TWI-type methods effectively alleviate some large RMSEs caused by the benchmark imputation methods and generally produce lower RMSEs. This shows the series imputed by TWI have marginal distributions that are stable (across time), meaning the method does not artificially induce structural shifts. This further corroborates the practical utility of TWI.

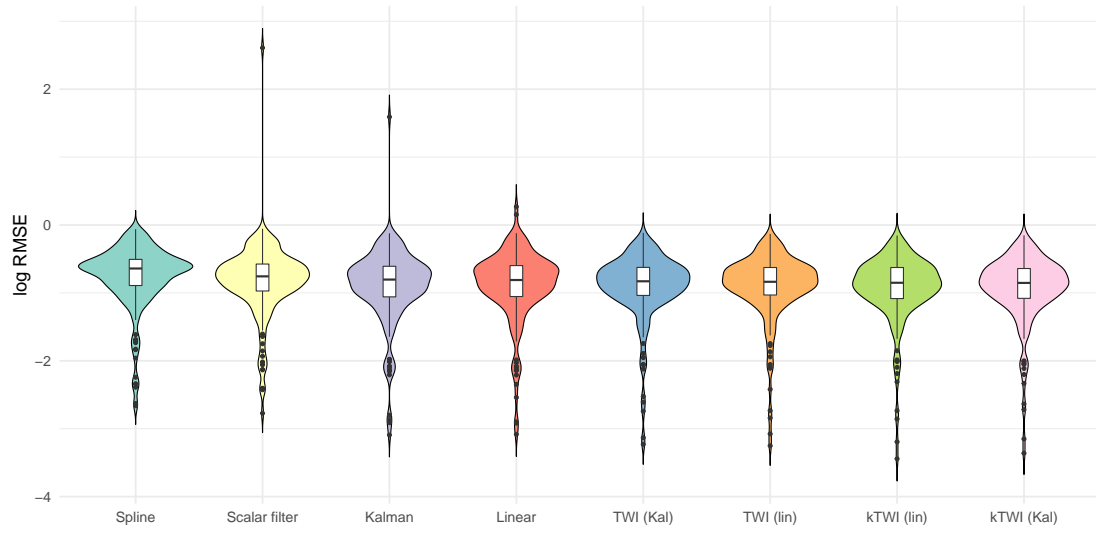


Figure S3: The distributions of the logarithm of the root mean squared prediction errors (RMSEs) for each method across the 176 series, ranked by median from left to right.